Low-albedo surfaces and eolian sediment: Mars Orbiter Camera views of western Arabia Terra craters and wind streaks

Kenneth S. Edgett

Malin Space Science Systems, Inc., San Diego, California, USA

Abstract. High spatial resolution (1.5 to 6 m/pixel) Mars Global Surveyor Mars Orbiter Camera images obtained September 1997 to June 2001 show that each of the large, dark wind streaks of western Arabia Terra originate at a barchan dune field on a crater floor. The streaks consist of a relatively thin (< 1 m) coating of sediment deflated from the dune fields and their vicinity. In most cases, this sediment drapes over a previous mantle that more thickly covers nearly all of western Arabia Terra. No concurrent eolian bedforms are found within the dark streaks, nor do any dunes climb up crater walls to deliver sand via saltation to the streaks. The relations between dunes, wind streak, and subjacent terrain imply that dark-toned grains finer than those that comprise the dunes are lifted into suspension and carried out of the craters to be deposited on the adjacent terrain. Previous eolian physics and thermal inertia studies suggest that, under modern Martian conditions, such grains likely include silt (3.9–62.5 μm), very fine sand (62.5–125 μm), and possibly fine sand (to ~210 μm). The streaks change in terms of extent, relative albedo, and surface pattern over periods measured in years; however, through June 2001, very little evidence for recent eolian activity (dust plumes, storms, dune movement) was observed.

received 18 July 2001, revised 21 December 2001,

accepted 2 January 2002, published 13 June 2002

Citation: Edgett, K. S. (2002) Low-albedo surfaces and eolian sediment: Mars Orbiter Camera views of western Arabia Terra craters and wind streaks, *Journal of Geophysical Research 107*(E6), 5038, doi:10.1029/2001JE001587.

Introduction

Low-albedo regions and surfaces on Mars have drawn scientific attention from the earliest telescopic views to the present. Since September 1997, high-resolution (1.5–15 m/pixel) Mars Global Surveyor (MGS) Mars Orbiter Camera (MOC) images have been highlighting the range of features that contribute to the properties of low-albedo surfaces on Mars (Edgett and Malin 2000, Malin and Edgett 2001); these include sand dunes, smooth-surfaced sand sheets, mantles (smooth-surfaced and, in some places, cracked coverings that drape over older, rugged terrain), dark ridge- and mesa-forming units associated with lighter-toned layer outcrops, and volcanic rock surfaces (Figure 1). Knowledge of low-albedo terrain aids our collective ability to interpret remote-sensing observations and select regions for future, more detailed study on the Martian surface. For example, on the basis of what was known about dark wind streaks in western Arabia Terra in 1994, the streak emergent from Trouvelot Crater (16°N, 13°W) was considered for a time as a second choice (after Ares Vallis) for the 1997 Mars Pathfinder landing because it was thought to be a sandy surface on which saltating grains would prevent dust from accumulating on rock surfaces (Edgett 1995, Golombek et al. 1997). Knowledge of the physical nature of dark spots and streaks in western Arabia is important because they are among the surfaces that provide some of the best thermal infrared spectral signatures (i.e., strongest absorption features) for interpretation of the planet's upper crust mineralogy, lithology, and eolian transport/ sorting processes (Wyatt et al. 2001). At present, remote infrared observations of Mars are the primary means for determining surface mineralogy from orbit, as indicated by the deployment of the Thermal Emission Spectrometer (TES) on MGS and the Thermal Emission Imaging System (THEMIS) on Mars Odyssey.

The purpose of this study was to use MOC images to test hypotheses proposed prior to the MGS mission regarding the genesis and physical nature of dark wind streaks in western Arabia Terra and to devise a current description of the streaks and their environs based on features observed. Figure 2 provides a regional view of the streaks; they each originate at a dark spot on the southern floor of an impact crater of 30–170 km diameter, many have bright margins, and all extend tens to a few hundred kilometers southeast or southwest. The streaks are large enough to be seen from Earth-orbiting telescopes (NASA and Hubble Heritage Team, images available at http://heritage.stsci.edu/public/2001jul/display.html) and have been the subject of more than a dozen

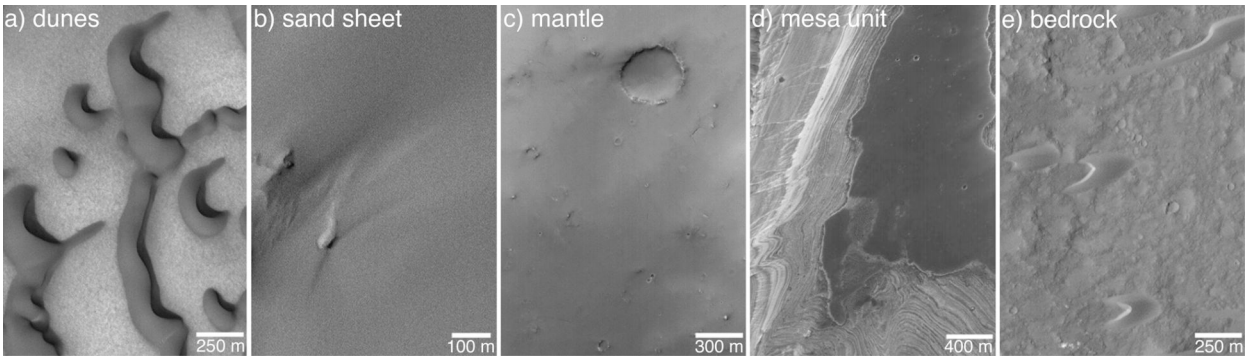

Figure 1. Mars Global Surveyor (MGS) Mars Orbiter Camera (MOC) views of the range of low-albedo surface types on Mars. **(a)** Sand dunes, north polar region, M00-01460, 76.6°N, 258.8°W. **(b)** Sand sheet, Gangis Chasma, M03-02943, 7.7°S, 49.5°W. **(c)** Smooth-surfaced mantle, Sinus Sabaeus, E02-00623, 6.9°S, 344.5°W. **(d)** Dark mesa-forming unit, west Candor Chasma, M18-01893, 6.3°S, 74.8°W. **(e)** Volcanic rock among eolian dunes at Meroe Patera, E04-01239, 7.1°N, 291.9°W. In each, illumination is from the left, and north is toward the top right.

scientific investigations spanning four decades (Sagan et al. 1972, 1973, Arvidson 1974, Soderblom et al. 1978, Thomas and Veverka 1979, 1986, Thomas et al. 1981, Peterfreund 1981, Kieffer et al. 1981, Thomas 1984, Presley 1986, McEwen 1987, Presley and Arvidson 1988, Henry and Zimbelman 1988, Strickland 1989, Arvidson et al. 1989, Mustard 1997, Cooper and Mustard 1998, Edgett and Malin 2000, Wyatt et al. 2001, Pelkey et al. 2001). A few similar streaks occur in neighboring Xanthe Terra and in the opposite hemisphere near Marte Vallis, Tartarus Colles, and Gale Crater (Thomas et al. 1981, Peterfreund 1981, Zimbelman 1986).

Data and Definitions

Data

Images of western Arabia Terra from Mars orbiters Mariner 9, Viking 1 and 2, and MGS were examined for this study. In particular, the research used MOC narrow-angle (NA) and wide-angle (WA) images acquired between 15 September 1997 and 30 June 2001. Because the MOC continued to collect data beyond June 2001, this paper is a "snapshot" of observations and deductions based only upon data obtained through that date. NA images were obtained at spatial resolutions ranging from 1.5 to 6 m/pixel to provide a combination of the highest resolution possible and longer images of slightly lower resolution, but improved signal to noise, designed to traverse across features of interest at similar solar illumination conditions. WA pictures studied include 240 m/pixel context images obtained when NA images were taken, 7500 m/pixel daily global map images, and other regional and local WA images between 240 and 7500 m/pixel.

Operation of MOC through the end of the Primary Mission on 31 January 2001 was described by Malin and Edgett (2001). Early Extended Mission operations in February 2001 through June 2001 were the same as in the Primary Mission, except MGS was occasionally commanded to roll off nadir so that MOC could acquire an image of a specific target such as a proposed Mars rover landing site. All data discussed in this report for the February–June 2001 period were obtained with the spacecraft in a nadir-looking orientation, and operations were conducted exactly as described by Malin and Edgett (2001) for the Mapping Mission. The pictures presented as figures in this report are subframes of the spacecraft images identified in the captions.

Definitions

Particle Size

Particle sizes are described in terms of the standard Wentworth (1922) sedimentology scale. The exception is the term "dust," which in Mars scientific literature refers to material of sizes < 10 μm and in most cases < 2 μm (Pollack et al. 1995, Tomasko et al. 1999).

Mantles

The term "mantle" refers to surficial sedimentary deposits of smooth texture (at pixel scales of 1.5–20 m) that drape over all, or all but the steepest, topography in a given terrain. Mantles cover and obscure roughness elements such as crater rims, small buttes, and hills. In plan view, mantles resemble air fall tephra deposits. Some mantles on Mars are many meters thick (Zimbelman and Greeley 1982, Schaber 1980, Christensen 1986). Unlike dunes or sand sheets (Figure 1), mantles have involved little or no ground transport and interaction with local topography; that is, mantles do not exhibit eolian bedforms and do not have tails nor depressions that arise in the lee of obstacles in environments of transport by saltation and traction (unless they have been eroded by wind, as observed on the Tharsis volcanoes by Malin and Edgett (2001)).

Tone and Albedo

The terms "dark-toned" and "light-toned" refer to the relative albedo of features in MOC images. NA data are not calibrated so as to provide a quantitative measure of albedo, and all the gray-scale images presented herein have been contrast-enhanced to emphasize

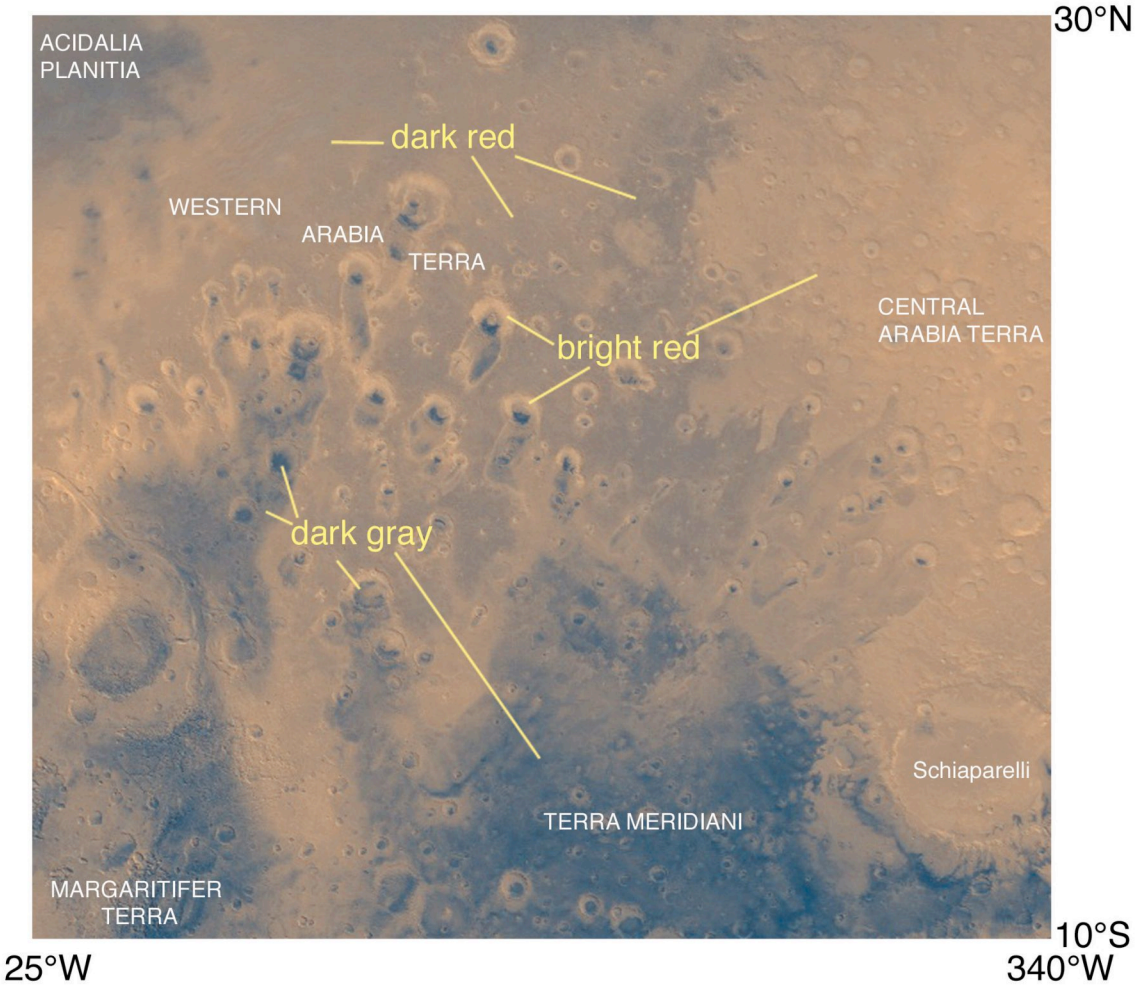

Figure 2. Western Arabia Terra: 153 craters have wind streaks (usually dark) that emanate from the south ends of craters and extend tens to over a hundred kilometers toward the south. The Viking "color units" of Presley and Arvidson (1988) and Arvidson et al. (1989) are indicated. Note that most dark wind streaks have a narrow bright red margin. The map is a mosaic of Viking orbiter images from the U. S. Geological Survey.

geologic and geomorphic detail. The term "albedo" is used in a similar, relative sense; quantitative albedos (i.e., wherein albedo is an indicator of intrinsic properties of materials on a planetary surface) have no bearing on the conclusions of this study.

Bedforms as Indicators of Saltation and Traction

The presence of eolian bedforms indicates that processes of saltation and traction have occurred at a given location. Absence of these landforms does not mean that these processes have not occurred, but the presence of the landforms mean that the processes definitely occurred. Eolian bedforms visible at MOC image scales include dunes and large ripples (or ripple-like bedforms). Dunes are composed largely of material in the particle size range most susceptible to movement via saltation, while ripples typically contain grains that are more difficult to set into motion (because they are larger or more dense) and thus move along as the result of the impact of saltating grains (traction). Under both terrestrial and Martian atmospheric conditions, sand-sized grains are most likely to saltate (Iversen and White 1982, Edgett and Christensen 1991). Ripple-like bedforms on Mars may be small dunes or very large ripples (Malin and Edgett 2001); large ripples on Earth have been called ripple ridges (Bagnold 1941), granule ripples (Sharp 1963), and megaripples (Greeley and Iversen 1985, p. 154). Such large ripples are most commonly found in areas from which most sand and finer grains have been deflated by wind to leave a lag of very coarse sand and granules; these coarser grains form ripples that are induced by impact of saltating grains as they move through an area and/or are dislodged and deflated from the surface.

Geologic and Geomorphic Setting

Western Arabia Terra is different from other parts of Mars because it has large, prominent wind streaks and

because the region includes all three basic Martian surface color "units" identified from Viking orbiter and telescopic views (Figure 2): "bright red," "dark red," and "dark gray" (Soderblom et al. 1978, Kieffer et al. 1981, McCord et al. 1982, Presley and Arvidson 1988, McEwen 1989, Arvidson et al. 1989). In terms of albedo, the three units are "bright," "intermediate," and "dark," respectively, relative to the average Martian surface (Viking Infrared Thermal Mapper albedos are 0.27–0.30 for bright red, 0.22–0.24 for dark red, and 0.14–0.17 for dark gray (Christensen 1988)).

By combining infrared and visible observations made from the Viking Infrared Thermal Mapper (IRTM) and visible imaging systems, a general view of western Arabia Terra emerged in which bright red surfaces were interpreted to consist of loose, bright dust; dark red surfaces were suspected of being older, immobile deposits of crusted dust; and dark gray surfaces were seen as places of active sand transport and/or bright dust removal (Presley and Arvidson 1988, Arvidson et al. 1989, Christensen and Moore 1992). Variants on this interpretation included the possibility that dark red surfaces are not necessarily crusted but are rougher than bright red surfaces (providing more shadows) at meter scale (Singer et al. 1984) and that bright red margins of the streaks resulted from erosional exposure or chemical alteration of dark, red, crusted materials (Kieffer et al. 1981, Mustard 1997).

The color, albedo, and thermophysical units of western Arabia were interpreted as "decoupled" from underlying bedrock, craters, and other landforms (Zimbelman and Kieffer 1979, Arvidson et al. 1989, Christensen and Moore 1992). The intercrater plains have been eroded and degraded such that there is an abundance (relative to other heavily cratered plains on Mars) of yardangs and remnant buttes and mesas of layered substrate (Presley 1986, Edgett and Parker 1997). A lack of small valley networks throughout western Arabia was seen as an indication that valley networks never formed there (Edgett and Parker 1997) or that erosion long ago removed their evidence (Hynek and Phillips 2001). Some large craters in western Arabia Terra were known to contain buttes and mesas of light-toned material that, at least in the case of Becquerel Crater (located at 22.2°N, 8.1°W), were interpreted to be layered (Thomas 1984). Subsequent MOC observations show that many western Arabia craters contain eroded, exposed, light-toned, layered rock units; and MOC images also confirm the layered nature of the intercrater terrain (Malin and Edgett 2000, 2001).

West Arabia Streak Genesis and Tests with MOC

A variety of wind streak forms have been modeled in wind tunnels and examined in the field on Earth (Greeley et al. 1974a, 1974b, Maxwell and El-Baz 1982, Greeley 1986, Greeley et al. 1989, Zimbelman and Williams 1996). In general, wind streak genesis involves all three modes of sediment transport, saltation, traction, and suspension, and a range of particle sizes from clay through granules. Wind streaks are recognized because their albedo (or roughness, if observed with radar) is somewhat different from that of their surroundings. This contrast results from some combination of eolian erosion and/or deposition. Recognition of a wind streak implies that the streak surface is physically different from the surface surrounding the streak; differences can be related to particle size, composition, color, presence of eolian bedforms, and/or vegetation. Thomas et al. (1981) classified the range and variety of Martian wind streaks; some are attributed to removal of fines in the lee of an obstacle, others are attributed to erosion of material everywhere except in an obstacle's lee, still others are thought to be caused by deflation of a material and subsequent deposition downwind of the source. Three different models for the origin of western Arabia streaks emerged prior to the MGS mission: (1) deflation, (2) deposition of grains moved via saltation and traction, and (3) deposition of grains transported in suspension.

Deflation

The Model

The deflation model contends that material has been removed by wind from the surfaces that are now expressed as dark streaks. Removal of dust was invoked to explain a variety of dark-toned Martian surface features, particularly those that changed and/or formed on timescales of days, weeks, and months over the course of the Mariner 9 and Viking missions (e.g., Sagan et al. 1973, Veverka et al. 1977, Thomas and Veverka 1979). Soderblom et al. (1978) and Kieffer et al. (1981) proposed that the dark streaks of west Arabia formed by deflation and exposure of a dark substrate. Both groups suggested that wind had eroded down through a surface covered by the dark red unit that pervades the region, exposing a stratigraphically lower dark gray unit. Bright red margins around each dark streak were proposed by Soderblom et al. (1978) to be a later mantle of dust superposed on, and maybe trapped along what they proposed to be a rugged, eroded contact between, the dark red and dark gray units. Kieffer et al. (1981), on the other hand, suggested that bright red margins represent a layer of dust that was exposed by deflation because it lies stratigraphically between the upper, dark red unit and the lower, dark gray unit.

Testing with MOC

In the absence of fieldwork, there is no foolproof method by which to test models for the genesis of wind streaks in western Arabia Terra. Analysis of MOC images and other remote-sensing data comes with all the caveats as with similar photogeologic work on Earth. Inferences made from analysis of aerial photographs of terrestrial wind streaks are usually found to lack important, sometimes unexpected, detail when investigated in the field. For example, the aerial visibility of a wind streak at Sleeping Beauty Mountain, California, was found to be modulated by the presence of annual changes in grass cover, and whether a particular grass grew on or off the streak was dependent upon the sediment and regolith properties of the streak and adjacent surface materials (Zimbelman

and Williams 1996). Despite the limitations of photogeology, there are specific features that can be sought and examined in MOC images that provide clues to genesis of Martian wind streaks.

To use MOC images to look for evidence of deflation as a cause for western Arabia streaks, one looks for eolian landforms common to deflation settings, such as megaripples, pedestal craters (formed by ejecta armoring of material otherwise subject to removal by wind), yardangs, and triangular remnants in the "shadow" or lee of decameter-scale obstacles (Malin and Edgett 2001). One also looks for clues (e.g., sharp, steep breaks in slope at streak/plains contacts) that the streak surface is topographically lower than surrounding terrain. These MOC tests only work if deflation has resulted in the characteristic landforms or proceeded to a depth of several meters so that the contact between deflated and non-deflated surfaces can be detected in a MOC image. If deflation has merely removed a thin coating of bright dust, a MOC image would not provide sufficient information unless the process of its removal was observed (for example, elsewhere on Mars, some Viking and MOC images show dust storms and dust devils actively removing thin coatings of bright material; and some Mariner 9, Viking, and MOC images show albedo changes that have occurred in periods of days, weeks, and months that can only be explained by removal of thin dust coatings).

Deposition via Saltation and Traction

The Model

The saltation and traction model proposes that grains deflated from an intracrater source have hopped (saltation) and rolled (traction) up the crater wall, over its rim, and downwind to a maximum distance at the distal terminus of the streak. On Earth, transport of saltating and rolling grains can produce wind streaks, tails, streamers, and bedforms (e.g., Maxwell and El-Baz 1982, Greeley et al. 1989, Zimbelman et al. 1995). Dark intracrater features of western Arabia were observed in early Viking IRTM data analyses to have thermal properties consistent with the presence of very coarse sand (Christensen and Kieffer 1979); subsequent studies found dunes in some of these craters and proposed that the dark streaks might result from deflation of finer sands, leaving coarser dunes and lag materials on the crater floors (Thomas et al. 1981, Christensen 1983, Presley 1986, Edgett 1995, Mustard 1997). High spatial resolution thermal inertia studies of the western Arabia streaks and the Pettit Crater streak near Marte Vallis (Zimbelman 1986; Henry and Zimbelman 1988, Mellon et al. 2000, p. 451, Pelkey et al. 2001) also concluded that they are predominantly composed of sand. The saltation deposition model was invoked to explain bright margins around the streaks by suggesting that saltating sand mobilizes bright dust and re-deposits this material along the streak margin (Thomas et al. 1981, p. 145). Alternatively, Mustard (1997) and Cooper and Mustard (1998) suggested that bright margins were created as saltating sand impinged upon a crusted dust/soil along the streak margin. A variant on the saltation deposition model suggests that sand might fine downwind toward the margins of each streak (Thomas et al. 1981). Fining downwind could occur by eolian sorting, attrition ("kamikaze effect" of Sagan et al. (1977)), or both. If sand grains fine downwind by breaking into smaller and smaller grains as they are bounced along the surface, then the length of each streak might be dictated by the distance grains can travel before becoming comminuted to particles small enough to be removed in suspension.

Testing with MOC

Evidence of saltation and deposition in streaks includes dunes, drifts, ripples, and/or thick eolian covers with streamers and swales indicating interaction of the streak material with topographic features in the area (e.g., patterns of interaction in the Gangis Chasma sand sheet, Figure 1b). Deflation of sand from an intracrater source would be evident in the form of drifts or dunes with slip faces indicative of transport in a direction that is up the crater wall and onto the terrain outside the crater. Further downwind, dunes and drifts would tend to accumulate at the downwind end of pits and hollows or in the lee of projections or lee-facing scarps. Because dunes are products of reduced transport energy, resulting in deposition of grains, dunes would be expected to occur (at least) at the margins of the wind streak, particularly at or near the distal end of each. Deflation could also have occurred as saltating grains abrade (and/or are removed from) the subjacent surface during transport down the length of the streak.

Deposition from Suspension

The Model

The suspension model proposes that grains deflated from an intracrater source were carried aloft by wind and deposited by falling to the ground. To the limit of Viking and Mariner 9 image resolutions available for the region (typically 100–250 m/pixel), Thomas and Veverka (1979) and Thomas et al. (1981) noted a lack of dunes within the western Arabia wind streaks. Thomas and Veverka (1979, p. 8143) further noted that the streaks appear to be relatively thin because, in some cases, their patterns changed (e.g., dark streaks lengthened) between Mariner 6 and Viking 2 and because the dark material "coats hills and flat places alike" as would a granular material deposited from suspension. In this model, fine, dark-toned grains are deflated from crater floors, raised to form plumes, and deposited downwind; bright margins reflect the finest grains deposited via this process.

Testing with MOC

Exploration of the suspension deposition model with MOC images involves both confirmation of an absence of forms attributed to saltation and deflation (sand dunes, drifts, ripples, yardangs, pedestal craters, etc.), and affirmation that subjacent surfaces have been draped by dark, streak-forming material. Contacts along the margins of the streaks might reflect this

mantling, as well, in which surfaces adjacent to the streak margins might appear more rugged or more cratered because they have not been covered with mantling material. In the most ideal case, a dust-raising event would be caught in the act of removing dark grains from an intracrater source, such as a dune field, and creating a plume of sediment that is blowing out over the streak. This process occurs on Earth; for example, satellites have captured plumes of dust generated by saltating sand impinging upon interdune soils and playas at the Great Sand Dunes of Colorado (Figure 3) and at White Sands, New Mexico (Gill et al. 2000). Martian dust storms usually consist of light-toned materials, but suspension of low-albedo fines in a dust storm was observed once in Terra Cimmeria by the Viking 1 orbiter (McEwen 1992).

West Arabia Wind Streak Type Example

Observations

A streak emanating from an impact crater located at 10.9°N, 347.8°W is a typical example of a western Arabia Terra dark streak (Figure 4). This streak was selected after examination of all MOC NA and WA images of the region. Figure 4a shows that NA views cover portions of the crater floor and dark streak. Figures 4b–4e sample the dark intracrater feature and wind streak along a single NA image, allowing comparison under similar illumination and atmospheric conditions.

The streak begins at a dark feature on the floor of the crater. The dark feature is a dune field (Figure 4b). The dunes are barchans, slip faces are on the south side of each, and a few have horns on their east sides that extend farther southward than horns on their west sides. Horns and slip faces indicate the dominant direction of sediment transport, which is the same direction indicated by the dark streak that extends southwestward from the crater (Figure 4a). The dunes were imaged twice, in September 1999 (Figure 4g) and September 2000 (Figure 4h). The dunes do not appear at this scale (6 m/pixel) to have moved, nor did discernable slip face avalanches occur, during the 0.55 Mars year interval between the two pictures.

The dune field does not extend all the way to the south crater wall, nor do any dunes climb the wall. The area in Figure 4b is the main concentration of dunes in the crater; about 9 km of dune-free space occurs between the dune field and the southern crater floor/wall interface toward which the dunes are or were

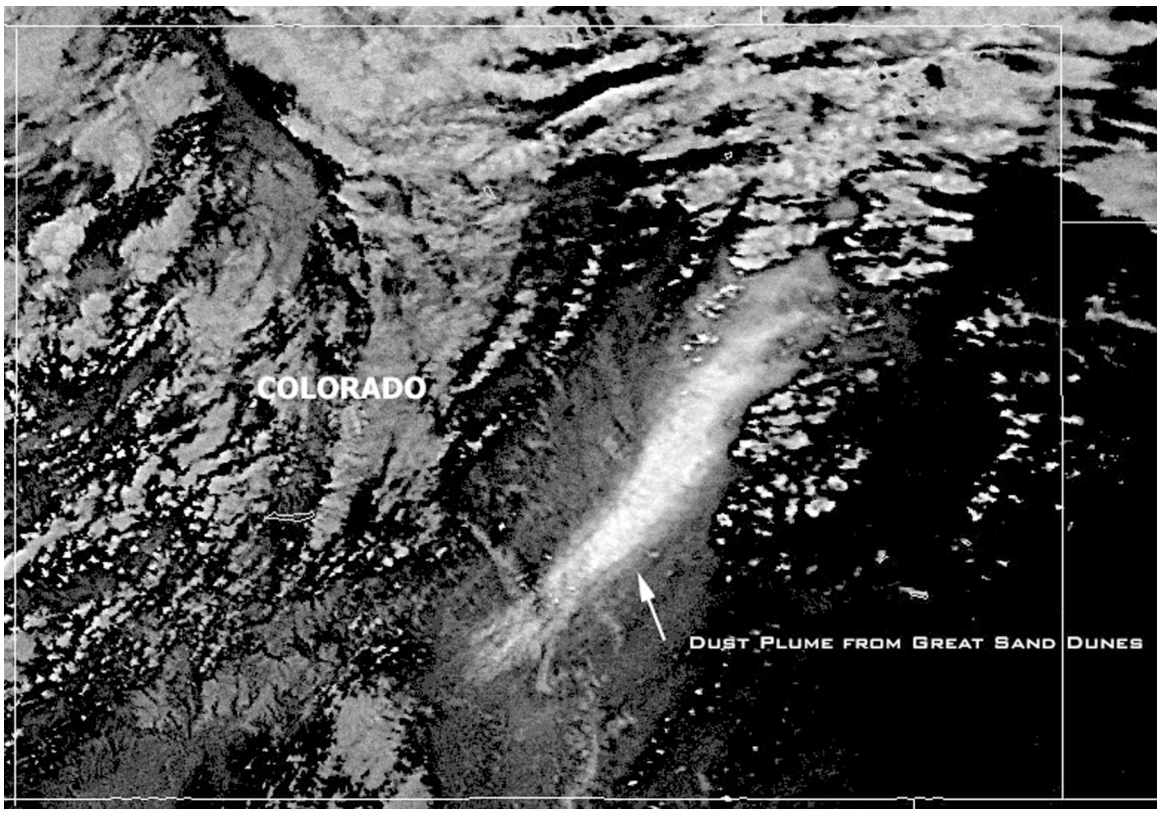

Figure 3. Dust plume emanating from the Great Sand Dunes National Monument, Colorado, on 18 April 2000 (2249 UTC); NOAA-14 Advanced Very High Resolution Radiometer image. Blowing sand impinging upon or being deflated from soils, playas, and other dust sources can lead to suspension and extension of plumes for tens to hundreds of kilometers downwind. The difference between bands 4 (10.3–11.3 μm) and 5 (11.5–12.5 μm) allows silicate particles in the plume to appear bright relative to H_2O clouds and land/lake surfaces. Image is courtesy of National Oceanic and Atmospheric Administration Operational Significant Event Imagery Team.

advancing. The crater wall is mantled by dark-surfaced material (Figure 4c). The mantle on the south crater wall is smooth (at 6 m/pixel), and this material drapes all but the steepest ridges near the crater rim at the south end of Figure 4c. The wall material is not as dark as the dune and interdune surfaces in Figure 4b, but the dark surface at the northeast (top right) corner of Figure 4c shows there is an abrupt change in albedo at the floor/wall interface. Outside the crater the dark streak surface is smooth; examples from the middle and southern margin of the streak are in Figures 4d and 4e, respectively. No dunes or ripples occur in the wind streak. In all cases, Figures 4c–4e, the surface is mantled such that low areas are filled in and somewhat flattened, high areas protrude above this smooth material and retain a rugged appearance at meter scales on their steeper slopes, and only a few small impact craters are present.

Each subframe of MOC image M07-06117 in Figures 4b–4e has been contrast-enhanced to show geomorphic detail, but the lower sixth of each was not processed so that the original appearance (relative albedo) is preserved. Each image in Figures 4b to 4e is located farther downwind than the previous. Note that the surface is darkest in Figure 4b and lightest in Figure 4e. Also note that the area preserved for "relative albedo" in Figure 4b is the interdune substrate surface; the dunes are darker still. What is observed, then, is a progression from the darkest material to lighter material: The dunes are darkest, the crater floor surrounding and immediately downwind of the dunes is lighter, the crater wall is lighter still, and the streak lightens from its proximal (near crater rim) to distal end.

The overall impression from Figures 4b–4e is that dark material (different from that which comprises the dunes) has mantled the surfaces downwind of the dune field to the distal end of the dark streak. MOC image E02-02843 furthers the case that dark streaks mantle underlying terrain. Figure 4f shows the portion of E02-02843 that crosses the bright margin of a wind streak immediately south of the crater at 10.9°N, 347.8°W. This streak actually emanates from the neighboring impact crater at 11.6°N, 346.7°W. The dark- and lighter-toned surfaces at the streak margin are somewhat different. Both surfaces are smooth at decameter scales but the light-toned surface at the streak margin and the intermediate-toned surface beyond the margin have irregularly shaped patches of intermediate-toned material (darker than the terrain beyond the streak margin) ranging in size from a few tens to a few hundred meters across. These patches are not visible in the dark wind streak, though they occur right up to its margin; these observations suggest that the intermediate-toned patches are superposed by the dark streak-forming material. As for the bright streak margin, it is only distinguished from adjacent terrain beyond the streak margin because it is brighter; there are no sharp albedo or topographic boundaries separating the dark material, nor the adjacent intermediate-toned plains, from the bright streak margin. These observations indicate that the bright margin may be composed only of a thin veneer of bright material (e.g., dust); the intermediate-toned patches within the bright margin may be physically rougher surfaces such that shadowing causes them to appear darker.

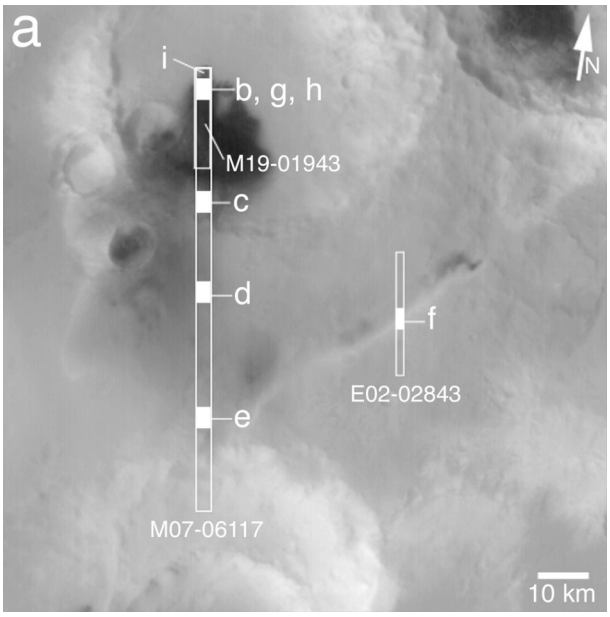

Figure 4. MOC views of a typical western Arabia dark streak. **(a)** Context view (M07-06118) of crater at 10.9°N, 347.8°W (top, center) with locations of narrow-angle (NA) images M07-06117, M19-01943, and E02-02843 indicated. Solid white rectangles indicate locations of subframes used in Figures 4b–4h. ***(Note: b–i are on subsequent pages.)*** **(b)** Dunes on crater floor in M07-06117. **(c)** Lower south crater wall in M07-06117. **(d)** Dark mantled streak surface in M07-06117. **(e)** Southern end of dark streak surface in M07-06117. **(f)** Dark streak (top), bright margin (middle), and adjacent terrain (bottom) in E02-02843. **(g, h)** Comparison of intracrater dunes in September 1999 (M07-06117) and September 2000 (M19-01943). The dunes did not move or change during this period. **(i)** Dunes trapped in small crater (top) on floor of the larger crater at 10.9°N, 347.8°W (M07-06117). Dark material covers the surface in a wedge-shaped region projecting southward from the intracrater dunes; this dark material obscures or reduces contrast between small light-toned bedforms (as seen to the right of the streak) and surrounding terrain. All pictures are illuminated from the left.

Interpretations

The wind streak emanating from the crater at 10.9°N, 347.8°W begins at the dune field. The streak likely has an origin connected with the dune field. Within the crater lies a miniature example of dark-toned sediment that has been transported downwind from dunes; Figure 4i shows two dunes trapped in a crater north of the main dune field in Figure 4b. A dark surface that is lighter in tone than the dunes widens outward and southward from the two trapped dunes; this surface mantles underlying light-toned ripple-like ridges that occur in depressions all around this dark area ("deflated material" in Figure 4i). The impressions offered by Figure 4i are (1) the dunes supply or are connected to material that generates the dark streak; (2) the dark the supply of streak is not

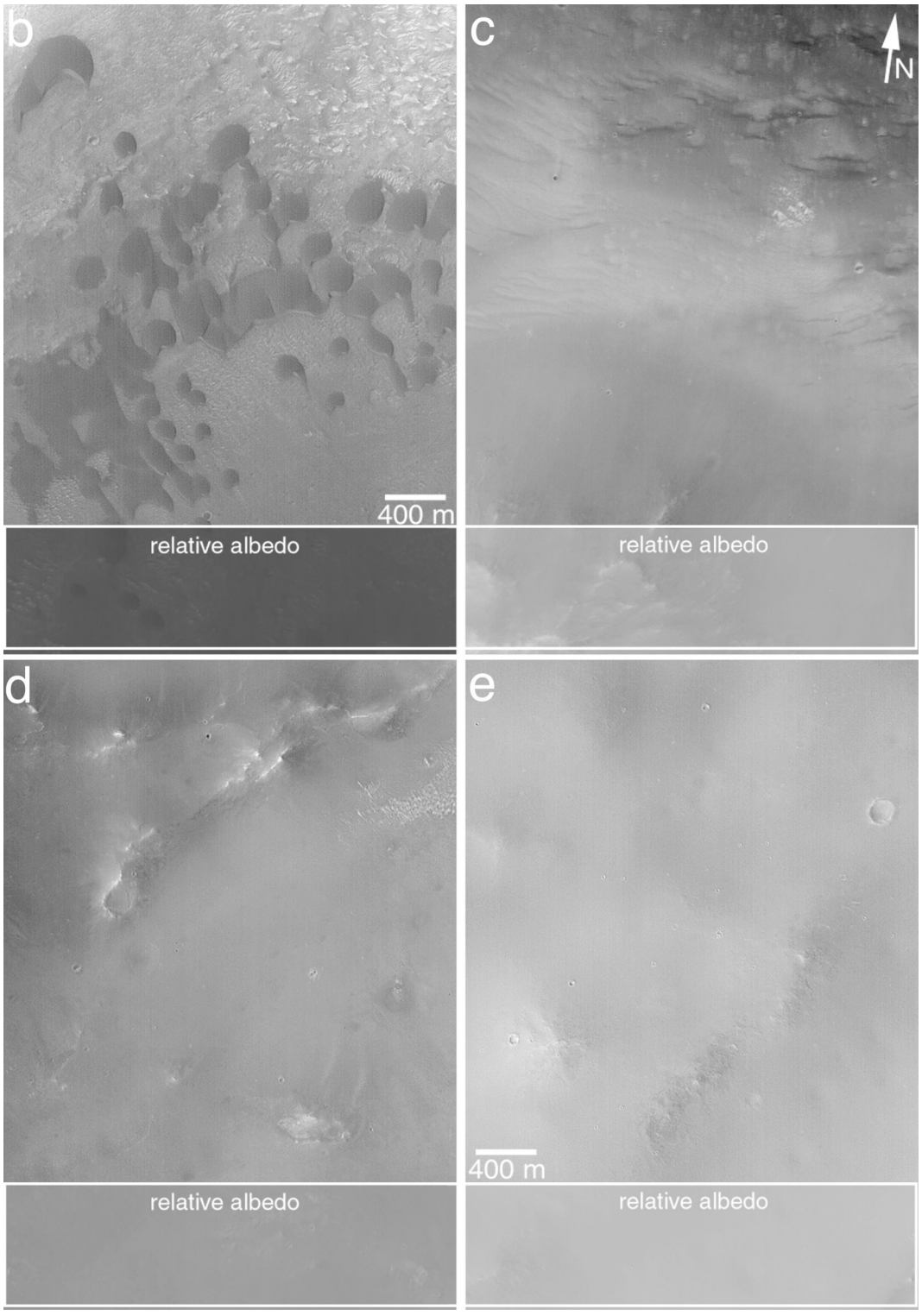

Figure 4, continued.

Figure 4, continued.

composed of material prone to collect in the shape of dunes or smaller bedforms like drifts and large ripples; (3) the streak is a thin deposit, because in some areas the lighter tone of the underlying ripple-like ridges is preserved; and (4) because the streak has a lighter tone than the dunes, it may be composed of something different from the dunes. At a larger scale, the same observations hold for the main wind streak in Figure 4a. The streak materials mantle underlying terrain. The streak is associated with the dunes: Either the dunes directly supply sediment to create the streak, or the streak materials are generated in the presence of the dunes (e.g., saltating dune sediments impact surrounding substrate material to create streak sediment). The brightening of the streak downwind suggests that something, perhaps particle size, changes downwind. These observations suggest that the streak consists of grains finer than those that comprise the dunes, the streak-forming grains are derived in the vicinity of the dunes, and they are deposited downwind of the dunes after being suspended in the atmosphere. The lack of bedforms large enough to be discerned in MOC images (e.g., dunes, large ripples) on the crater wall and throughout the wind streak are good indicators that saltation and traction have not been as important as suspension in transporting dark granular materials to create the streaks. Observations of the type example, therefore, support the suspension deposition model for streak genesis in western Arabia Terra.

Observations and Interpretations Regarding All West Arabia Streaks

Not all wind streaks and their adjacent craters in western Arabia Terra are exactly alike, but all share attributes of the type example. What follows is a description of MOC observations regarding the interiors of craters from which streaks emanate, the terrain that surrounds the craters and upon which the streaks are superposed, the surfaces of the streaks, and evidence for eolian activity in western Arabia Terra.

Crater Interiors

Dark-toned Landforms and Surfaces

Within each crater from which a wind streak emanates, there are three different dark-toned surfaces; and in some cases, there is a fourth. The three that all share are (1) dunes, (2) interdune and crater floor surfaces, and (3) a darkened crater wall downwind of the dunes. The fourth are dark mesa-forming units; these are not found in all craters that have dark wind streaks and dunes.

As noted, the typical western Arabia wind streak begins at a dune field on a crater floor (Figure 4). Through June 2001, 116 MOC NA images of dark intracrater features in western Arabia Terra were acquired. These images cover portions of 48 of the 153 total dark intracrater spots in the region, and most that have not been imaged are the smallest (< 10 km wide) dark spots. Table 1 lists the first image acquired by any spacecraft that showed a dune field within 43 of the 48 dark intracrater spots in western Arabia Terra. As with the example in Figure 4, the dune fields consist of barchans located more than a few kilometers north of the southern crater walls, and all have slip faces pointed in the same direction indicated by the adjacent

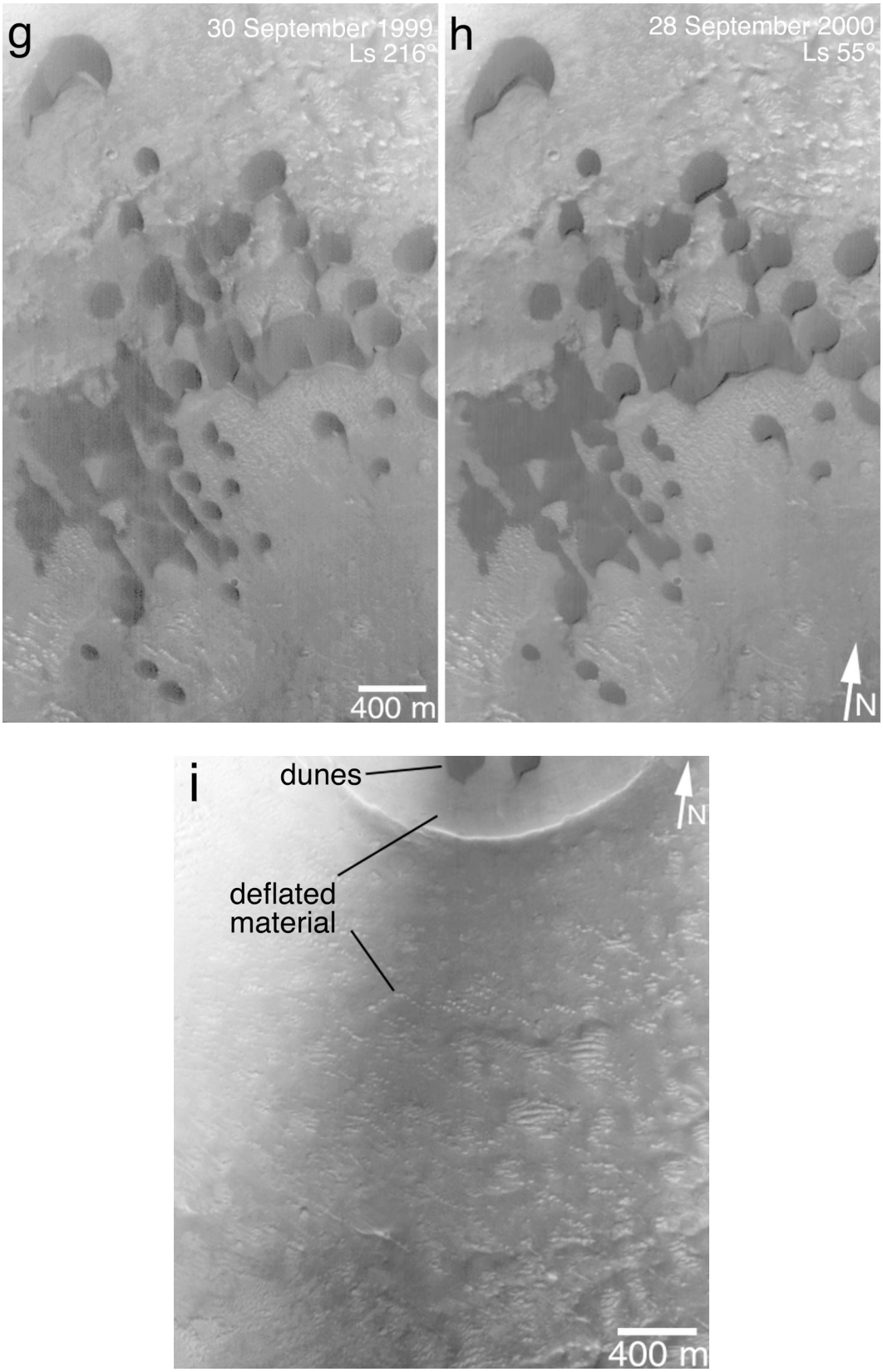

Figure 4, continued (final).

Table 1. Craters With Dunes at Wind Streak Source in Western Arabia Terra From Images Acquired Through June 2001

Location		Earliest Picture Showing Dunes		
Latitude	**Longitude**	**Spacecraft**	**Image Number**	**Year**
11.3°N	346.8°W	Mariner 9	DAS 9449589	1972
22.2°N	8.1°W	Viking 1	209A07	1977
17.2°N	4.9°W	Viking 1	2I2A45	1977
8.9°N	348.9°W	Viking 2	411B14	1977
11.0°N	2.9°W	Viking 1	708A03	1977
1.7°N	351.7°W	Viking 1	709A42	1978
8.0°N	7.0°W	Viking 1	369S34	1980
4.2°N	5.4°W	MGS	AB1-03001	1997
11.0°N	350.9°W	MGS	SP1-26004	1998
22.1°N	22.5°W	MGS	SP2-34903	1998
13.1°N	3.6°W	MGS	SP2-35103	1998
6.7°N	345.8°W	MGS	SP2-40803	1998
21.3°N	17.5°W	MGS	SP2-42304	1998
19.2°N	10.7°W	MGS	SP2-44207	1998
15.5°N	22.2°W	MGS	SP2-5I303	1998
16.4°N	13.1°W	MGS	SP2-53203	1998
8.3°N	358.7°W	MGS	M03-02407	1999
5.0°N	10.2°W	MGS	M03-02716	1999
2.3°N	7.8°W	MGS	M03-05599	1999
2.7°N	358.9°W	MGS	M03-06290	1999
13.2°N	18.0°W	MGS	M04-02192	1999
24.6°N	10.8°W	MGS	M04-02970	1999
16.5°N	16.5°W	MGS	M07-00748	1999
2.7°N	9.4°W	MGS	M07-02411	1999
5.7°N	351.5°W	MGS	M07-05541	1999
11.0°N	347.8°W	MGS	M07-06117	1999
10.9°N	1.4°W	MGS	M08-05219	1999
10.1°N	351.9°W	MGS	M11-00086	2000
18.2°N	17.0°W	MGS	M11-00431	2000
13.8°N	23.3°W	MGS	M11-01942	2000
14.9°N	359.0°W	MGS	M20-01694	2000
7.4°N	353.1°W	MGS	M21-00827	2000
10.9°N	4.4°W	MGS	E02-01145	2001
9.2°N	347.7°W	MGS	E02-01236	2001
13.6°N	20.1°W	MGS	E02-02645	2001
12.5°N	0.8°W	MGS	E04-00599	2001
13.8°N	9.8°W	MGS	E04-01032	2001
14.9°N	19.0°W	MGS	E04-01271	2001
16.5°N	15.3°W	MGS	E05-00437	2001
11.0°N	14.0°W	MGS	E05-01993	2001
14.6°N	14.9°W	MGS	E05-01995	2001
13.1°N	7.2°W	MGS	E05-02644	2001
8.5°N	15.8°W	MGS	E05-03231	2001

dark wind streak. All of the dunes are dark-toned and darker than the wind streaks. In some craters, eolian bedforms smaller and lighter-toned than the dunes occur in isolated troughs and depressions; in some cases, the darker dunes have overridden the lighter-toned bedforms (Edgett and Malin 2000, Fig. 24, Malin and Edgett 2001, Fig. 38).

Not all dark intracrater spots exhibit dune fields (Table 2). While the list is short (five locations), four of the dark intracrater features in Table 2 have something in common: They do not have a dark wind streak. The remaining one on the list has a wind streak, but MOC coverage is not adequate to be certain that no dunes are present. An example that has no wind streak and no dunes is the dark spot in Curie Crater (Figure 5). Two NA images cover portions of the dark spot in Curie Crater, and neither exhibits dunes, although dark patches of sediment can be seen filling small pits and craters. In Curie Crater, there may be an insufficient amount of material to form dunes. Alternatively, it is possible that dunes are present in Curie, but a picture of them has not yet been acquired.

Some of the dark material on crater floors in western Arabia Terra are not dune fields nor are they like the dark surfaces in Curie Crater. Figure 6 shows a portion of the low-albedo surface in Crommelin Crater at 5°N, 11°W; the dark material in this case is a smooth-surfaced steep-sided mesa-forming unit that overlies a rugged, lighter-toned material seen in windows through the dark mesa-forming unit (note, however, that Crommelin and similar craters also have dark dune fields; Table 1). Dark mesa-forming units, first described by Malin and Edgett (2000), are most common in craters along the southern margins of western Arabia Terra; that is, they are in craters closest to Terra Meridiani (Figure 7). Indeed, along the northern margins of Terra Meridiani, dark mesa-forming units can be found on the intercrater plains, as well. The rugged appearance of the underlying light-toned unit implies that the dark mesa-forming unit was emplaced after the light-toned material achieved its rugged appearance (i.e., the dark mesa-forming unit lies unconformably on a previously eroded surface).

Light-toned Layer Outcrops

Light-toned layered outcrops are most common and more extensive in craters closest to the light-toned, layered, intercrater outcrops of northern Terra Meridiani (Figure 7). Craters farther from Terra Meridiani have smaller layer outcrops, such as the isolated features in Trouvelot and Becquerel Craters (Figure 8), and many others away from Terra Meridiani have no such outcrops, such as Curie Crater (Figure 5). The layer units exhibit cliff-bench morphology, preserve faults and fault offsets, and in most cases are of similar thickness from one layer to the next (Figure 9a). Some layer outcrops are the source of light-toned material that has been shed to form light-toned wind streaks (Figure 9b). MOC images of the layers in Becquerel Crater show that some layers are dark-toned, but these are not as dark as the dunes within the crater (Figure 9c). The morphologic characteristics of the layer outcrops suggest they are indurated materials; the repeated thickness suggests repeated changes in their depositional environment; and the shedding and eolian transport of bright grains suggests their particles sizes are fine.

Other Crater Interior Surfaces

Other surfaces within western Arabia impact craters are smooth at hectometer scale but rugged and craggy at decameter scale (Figure 10a). In some cases, the rugged and craggy crater floors result from deflation, as indicated by the presence of pedestal craters (Figure 10b). Other crater interior surfaces, especially crater walls that are not subjacent to the dark wind streaks, are thickly mantled by materials that have smooth, intermediate-toned surfaces (Figure 10c).

Surrounding Terrain

Surface Materials

The upper surface material of most of western Arabia Terra, that which gives the region its distinctive "dark red" color, is a mantle deposit (Figure 11). The mantle is thinner than mantles on crater rims (e.g., Figure 10c) and may be no more than a few meters thick (Figure 11). Christensen and Moore (1992) predicted on the basis of thermophysical properties that the surface in

Table 2. Craters with Dark Intracrater Spot Lacking Dunes in Western Arabia Terra Images Through June 2001

Location			
Latitude	**Longitude**	**Relevant MOC Pictures**	**Observations and Comments**
27.0°N	16.9°W	E04-01503	No wind streak; dark spot has no dunes.
29.0°N	4.7°W	M08-03017 and E04-01360	No wind streak, no dunes; Curie Crater.
17.3°N	354.0°W	M03-04393	No wind streak; small dark patches may be drifts of sand, but no dunes present.
16.0°N	354.7°W	M11-01924 and M23-01170	No wind streak; small dark patches may be drifts of sand, but no dunes present.
2.l°N	349.5°W	M11-01157	Has wind streak; small dark patches may be drifts of sand, coverage may not be complete enough to see larger dunes.

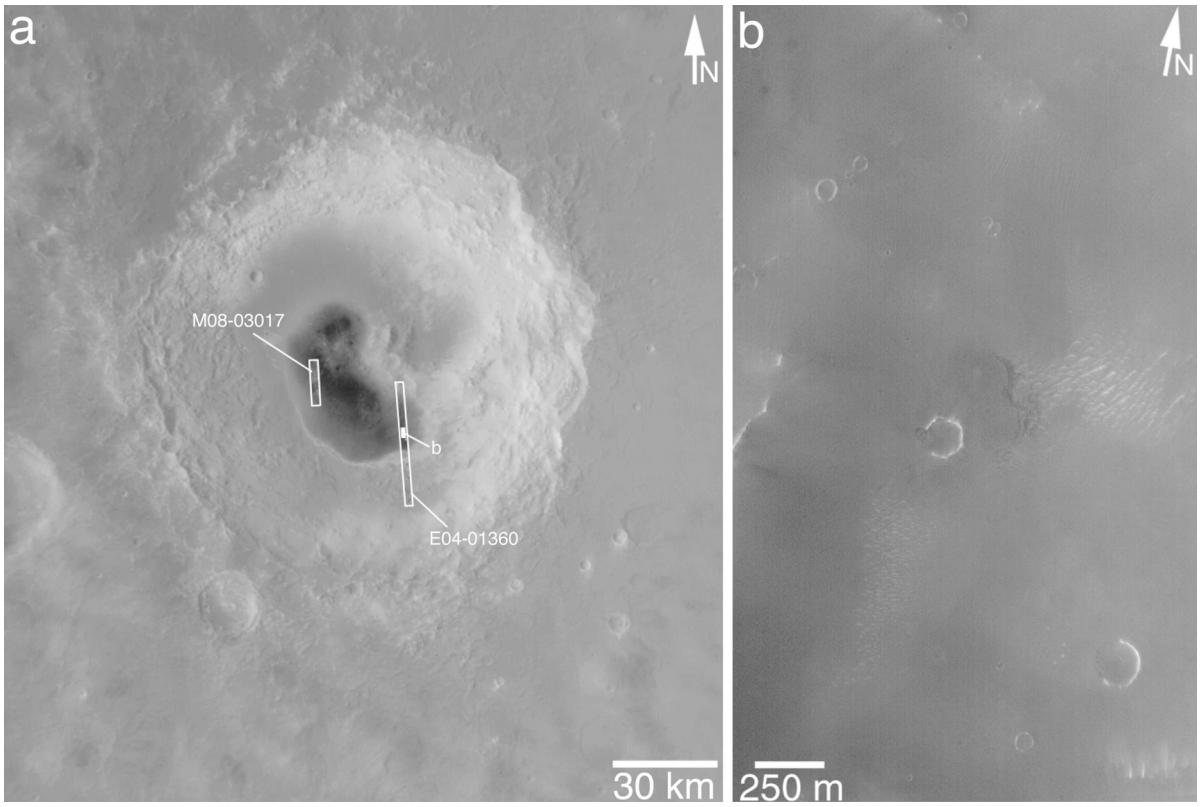

Figure 5. Curie Crater dark spot, 29.1°N, 4.8°W. **(a)** Context view, from MOC M01-01240, showing Curie Crater, its dark spot, and location of the two NA images of the dark spot. No dunes are present in either NA image. Patchy clouds obscure portions of the south and west parts of the context view. **(b)** Detailed view of dark spot surface in E04-01360. Both pictures are illuminated from the bottom left.

this region would be mantled; following Presley and Arvidson (1988), they predicted that the mantle would be crusted and might represent a stratigraphically older mantle than the high-albedo material covering most of central Arabia Terra. Whether the dark-red-surfaced mantle is indurated is not known, as there are no obvious features in MOC images that would indicate that the material is indurated.

Substrate and Subsurface Materials

The substrate beneath the mantle that covers most of western Arabia is layered. Evidence for layering can be seen, for example, in Figures 12 and 13. Erosion that predates the mantling of the region by dark-red-surfaced material has exposed and expressed the layered substrate as terraces, pedestal craters, and yardangs. In the far western areas around Mawrth Vallis the substrate is not mantled and reveals dark mesa-forming units overlying light-toned layered units (Malin and Edgett 2000). Along the margin of the streak emanating from Rutherford Crater, similar dark mesa-forming units and light-toned substrates are exposed (Figure 14). In the case of the Rutherford streak, the light-toned substrate and dark mesa-forming material do not comprise the streak; rather, the material that gives the overall streak its dark tone is a thin veneer superposed on these surfaces.

Streak Surfaces

Variety and Comparison to Viking

Thomas and Veverka (1979) observed that the wind streaks in western Arabia change in terms of length and albedo relative to surrounding terrain on timescales short enough to have been observed between the Mariner 6 (1969), Mariner 9 (1972), and Viking orbiter (1976–1980) missions. Consistent with this observation, many streaks are different in MOC WA views than they were when seen by the Viking orbiters. Figure 15 documents four basic types of changes. Relative to their surroundings, some streaks are about the same as they were during the Viking mission, others became lighter, others disappeared, and others grew longer. Little or no change occurred September 1997 through June 2001.

Dark Streak Surfaces

At decameter scale, wind streaks of western Arabia Terra have smooth surfaces. In no cases are the streaks composed of or contain eolian bedforms. In cases where ripples or ripple-like features are present in the streaks (as observed by Edgett and Malin (2000) in MOC image AB1-03001), they are covered by mantling material and oriented differently than the

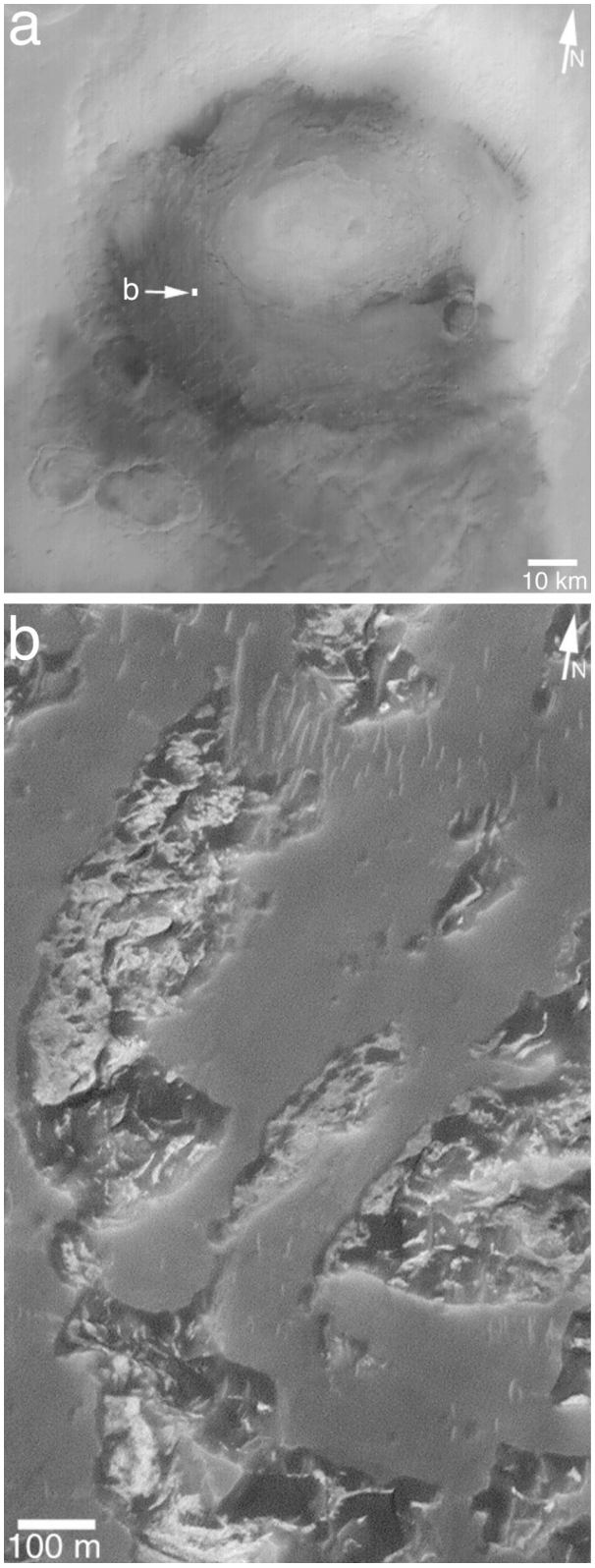

Figure 6. Dark mesa-forming unit in western Crommelin Crater. **(a)** Context showing Crommelin Crater, located at 5.1°N, 10.3°W, MOC WA image M20-00871. **(b)** High-resolution view, showing smooth-surfaced dark mesa-forming unit overlying light-toned, rugged surface of layered outcrops materials, image M20-00870. Both pictures are illuminated from the left/top left.

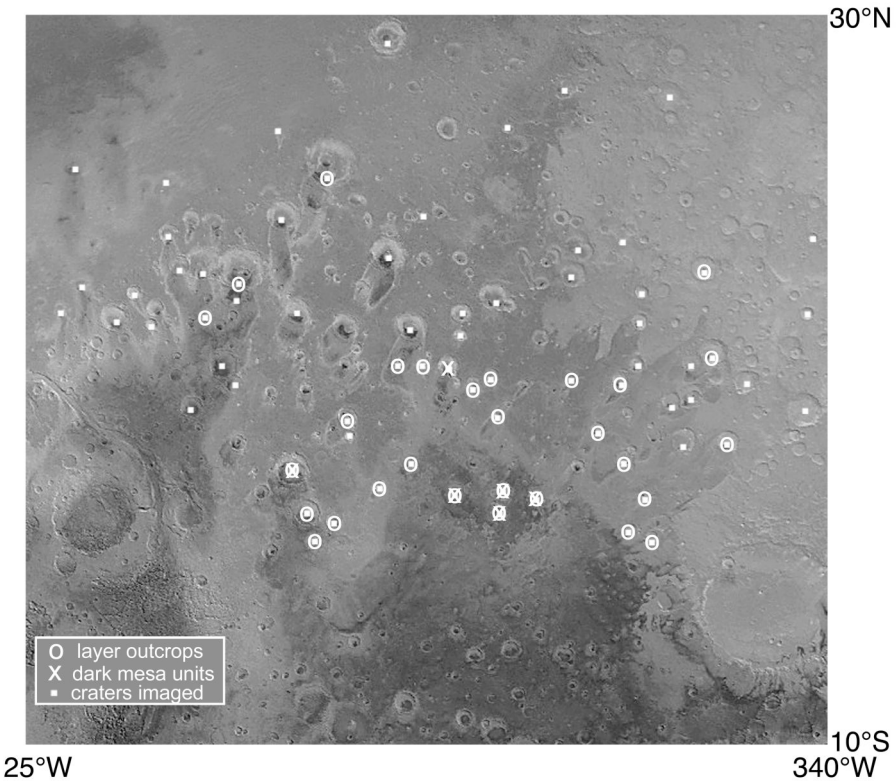

Figure 7. Crater interiors in western Arabia Terra that exhibit light-toned layering (circles) and dark mesa-forming units (crosses). For reference, craters in which at least one MOC NA image was obtained through June 2001 are indicated by small squares. Base map is a mosaic of Viking orbiter images from the U. S. Geological Survey.

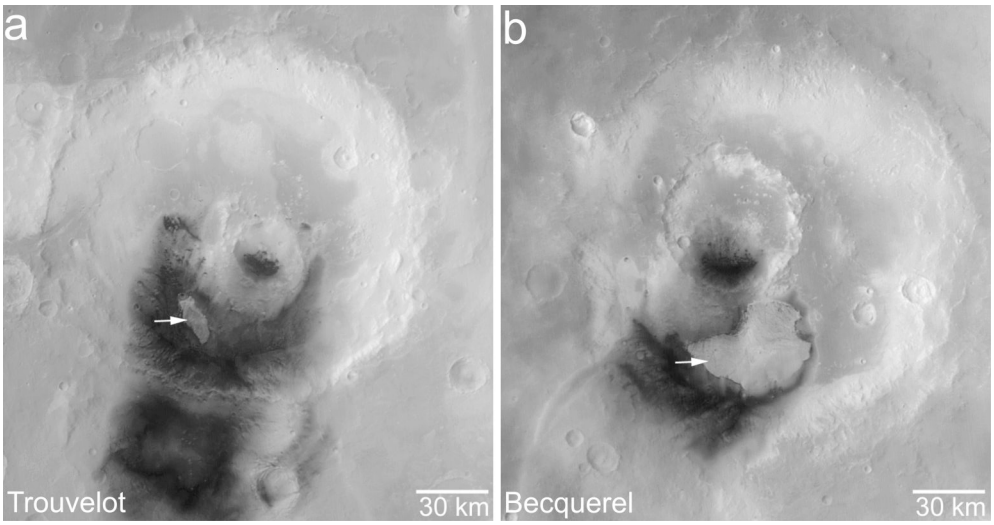

Figure 8. Light-toned layer outcrop mounds (arrows) in **(a)** Trouvelot Crater (16.3°N, 13.0°W; mosaic of MOC M01-00459, M01-01444, M01-01446) and **(b)** Becquerel Crater (22.3 N, 8.3 W; MOC M01-00849). North is up; illumination is from the left.

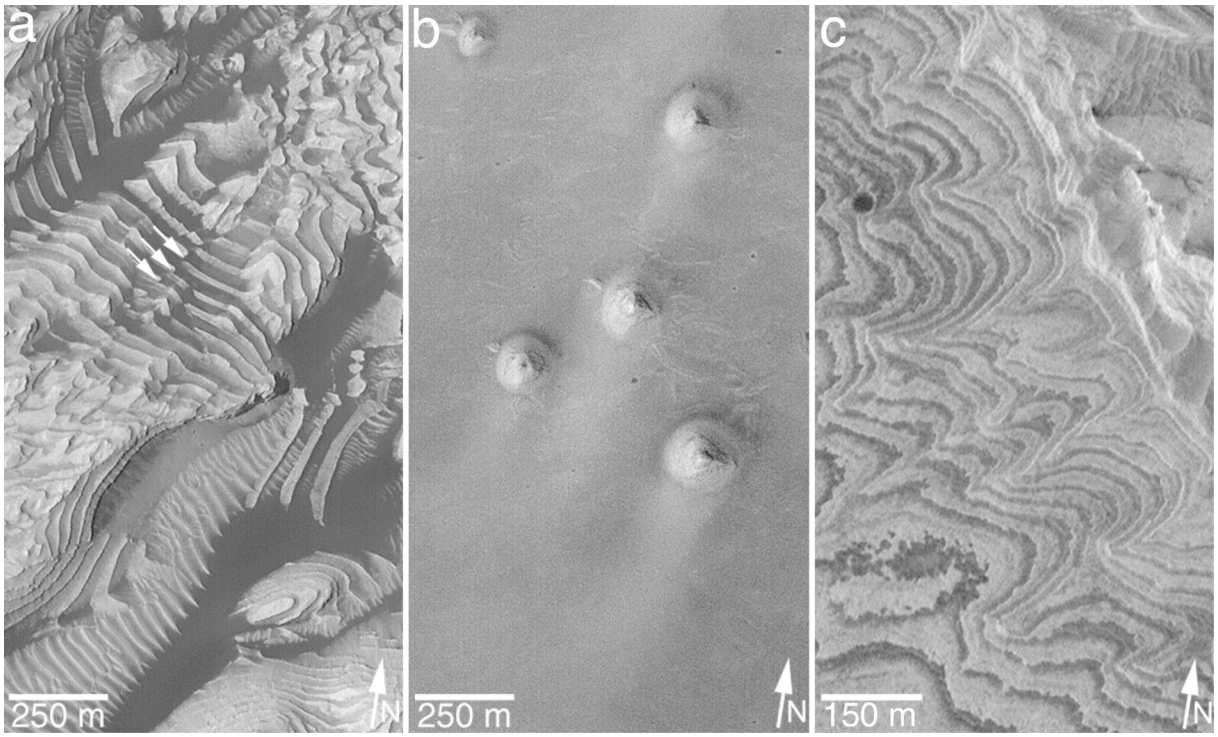

Figure 9. (a) Detail of light-toned layer outcrops in crater at 8°N, 7°W. Arrows indicate a fault across which cliff-bench layer exposures are offset. Dark sand drifts accentuate contrast between layers. MOC image E05-00804 is illuminated from the left/bottom left. **(b)** Light-toned layered outcrops in western Arabia Terra craters as a local source for light-toned sediment. This example is in a crater at 2.2°N, 7.8°W; the picture shows that light-toned wind streaks shed directly from adjacent light-toned buttes. MOC image M09-06275 is illuminated from the bottom left. **(c)** Erosion exposing alternating light- and dark-toned layers in the Becquerel Crater layered mound (Figure 8b). The dark-toned layers are about as dark as the eolian megaripples visible at the right and top right but are not as dark as sand dunes and drifts seen elsewhere in the full MOC image, M03-03117, from which this subframe was cut. Dunes in Becquerel are typically as dark as the darkest feature shown here, a circular depression (near top left). Centered near 21.6°N, 8.2°W, this scene is illuminated from the bottom left.

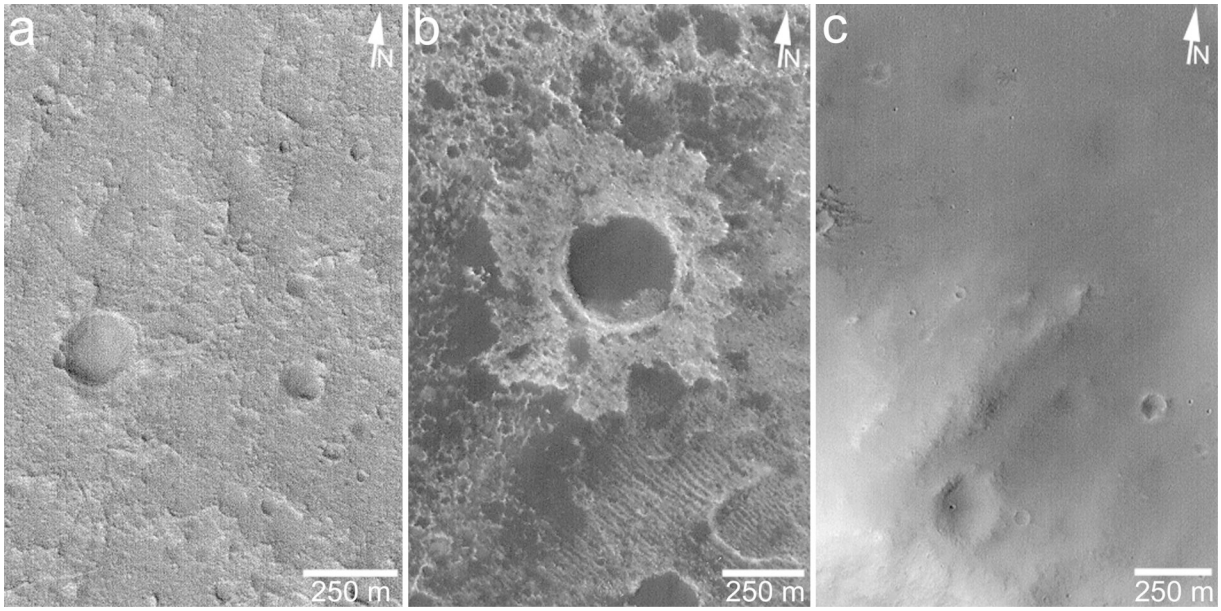

Figure 10. MOC views of typical western Arabia Terra intracrater surfaces outside dune fields and layered units. All examples are from Trouvelot Crater (Figure 8a). **(a)** Rugged and craggy crater floor near 16.8°N, 13.6°W, M08-07400. **(b)** Pedestal crater formed by deflation of layer immediately beneath the crater ejecta, which served as a rocky armor to protect the underlying material from removal, near 15.9°N, 13.4°W, E05-01291. **(c)** Typical crater wall and rim surfaces mantled by smooth-surfaced, intermediate-toned material; this example is near 17.5°N, 12.9°W, in M02-01093. All images are illuminated from the left.

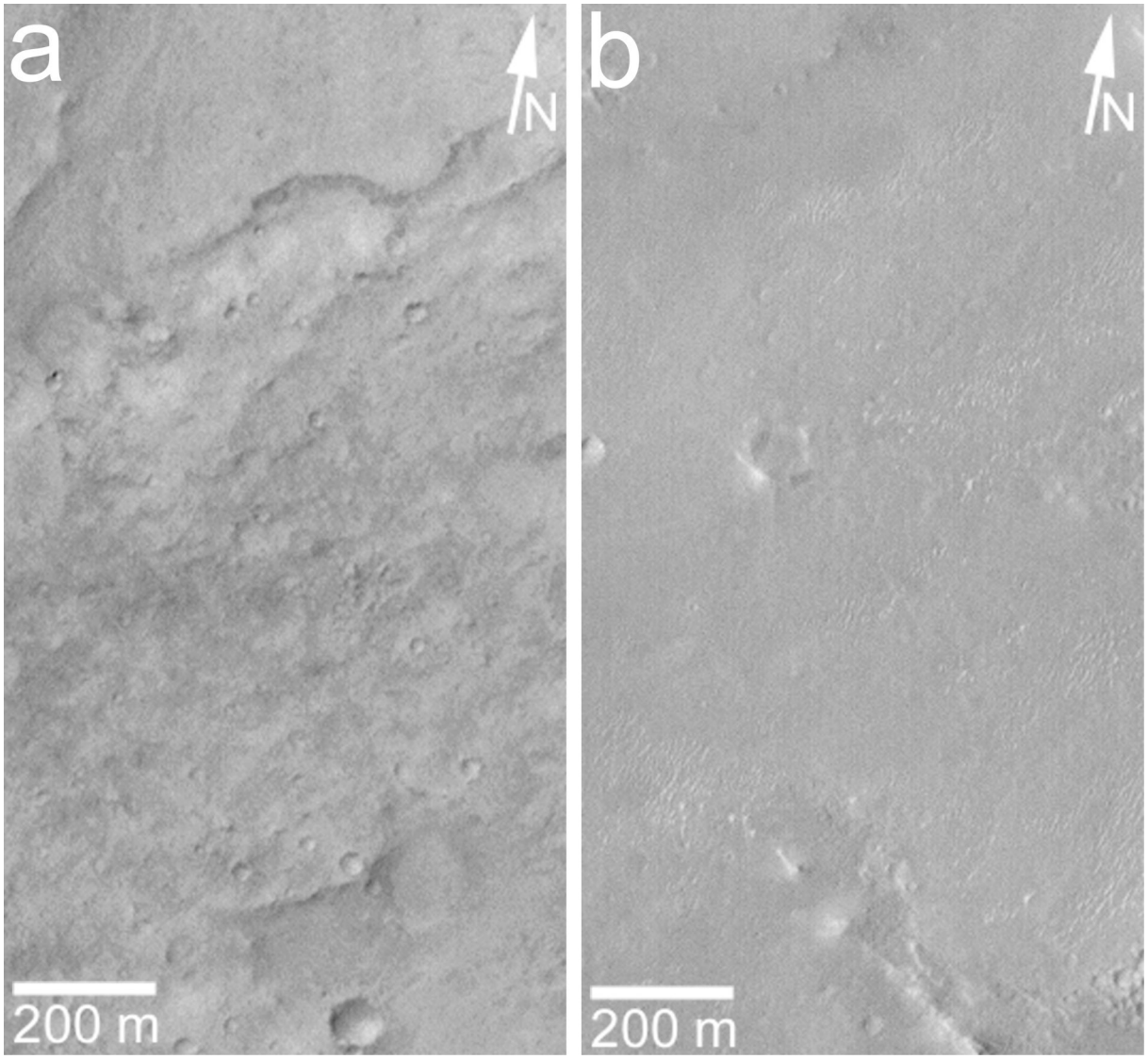

Figure 11. Typical western Arabia Terra intercrater plains mantled by a material that, at the surface, presents the "dark red'' color and intermediate albedo described by researchers working with Viking data prior to the MGS mission (e.g., Arvidson et al., 1989). **(a)** Example near Trouvelot Crater at 15.7°N, 11.5°W; MOC CAL-00425. **(b)** Example near 7.5°N, 354.2°W; MOC M03-02924. Both images are illuminated from the left.

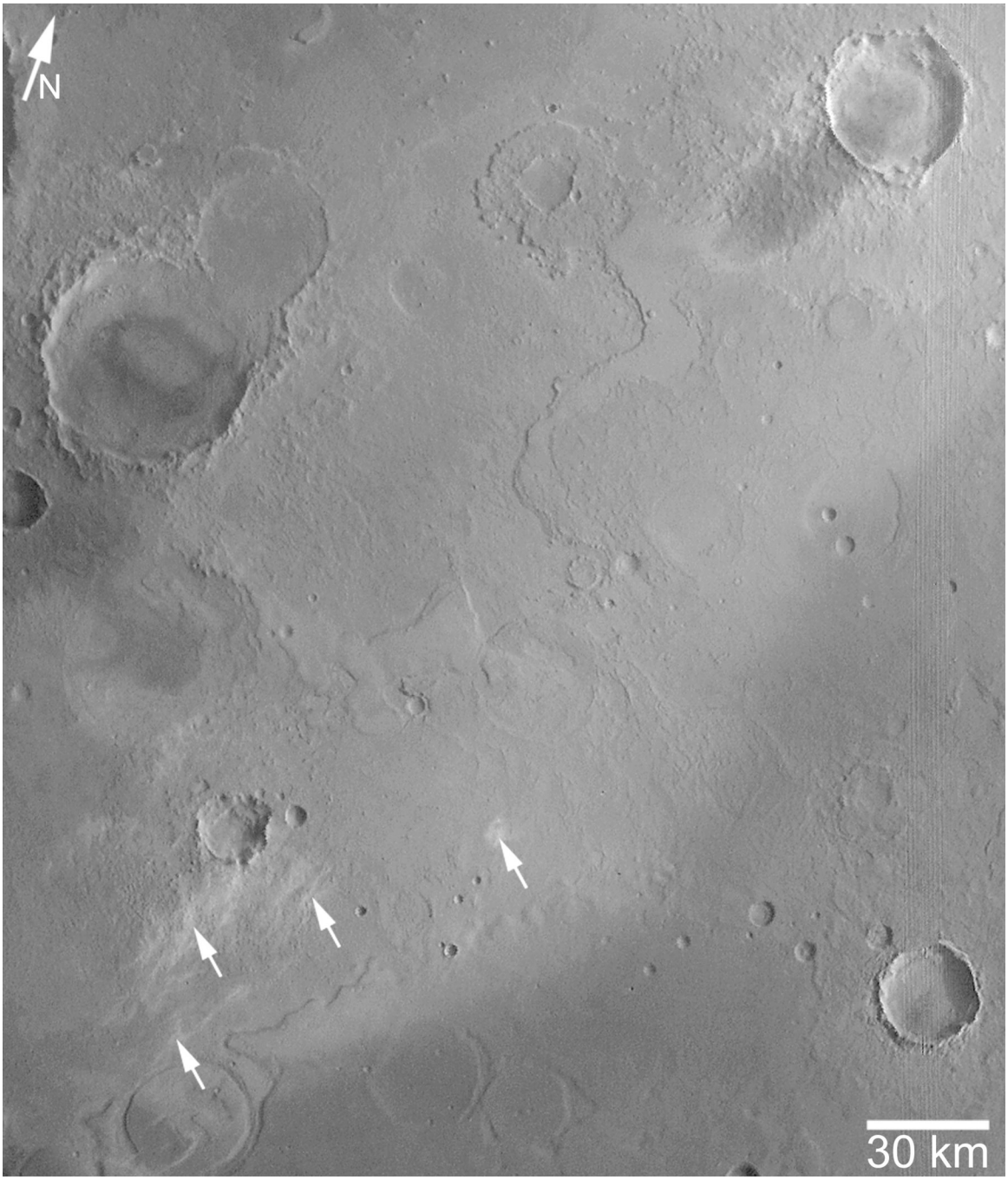

Figure 12. Layered intercrater terrain of western Arabia Terra and dust plumes (arrows) observed on 1 April 1978 by Viking 1. No dust plumes were evident on or near the wind streaks or intracrater dune fields (e.g., top right corner). The terraced nature of the intercrater plain (especially near image center) indicates layered substrate exposed by erosion that predates the surficial mantles that presently cover the region (Figure 11). Portion of 653A58, with center near 1.9°N, 6.0°W, is illuminated from the right.

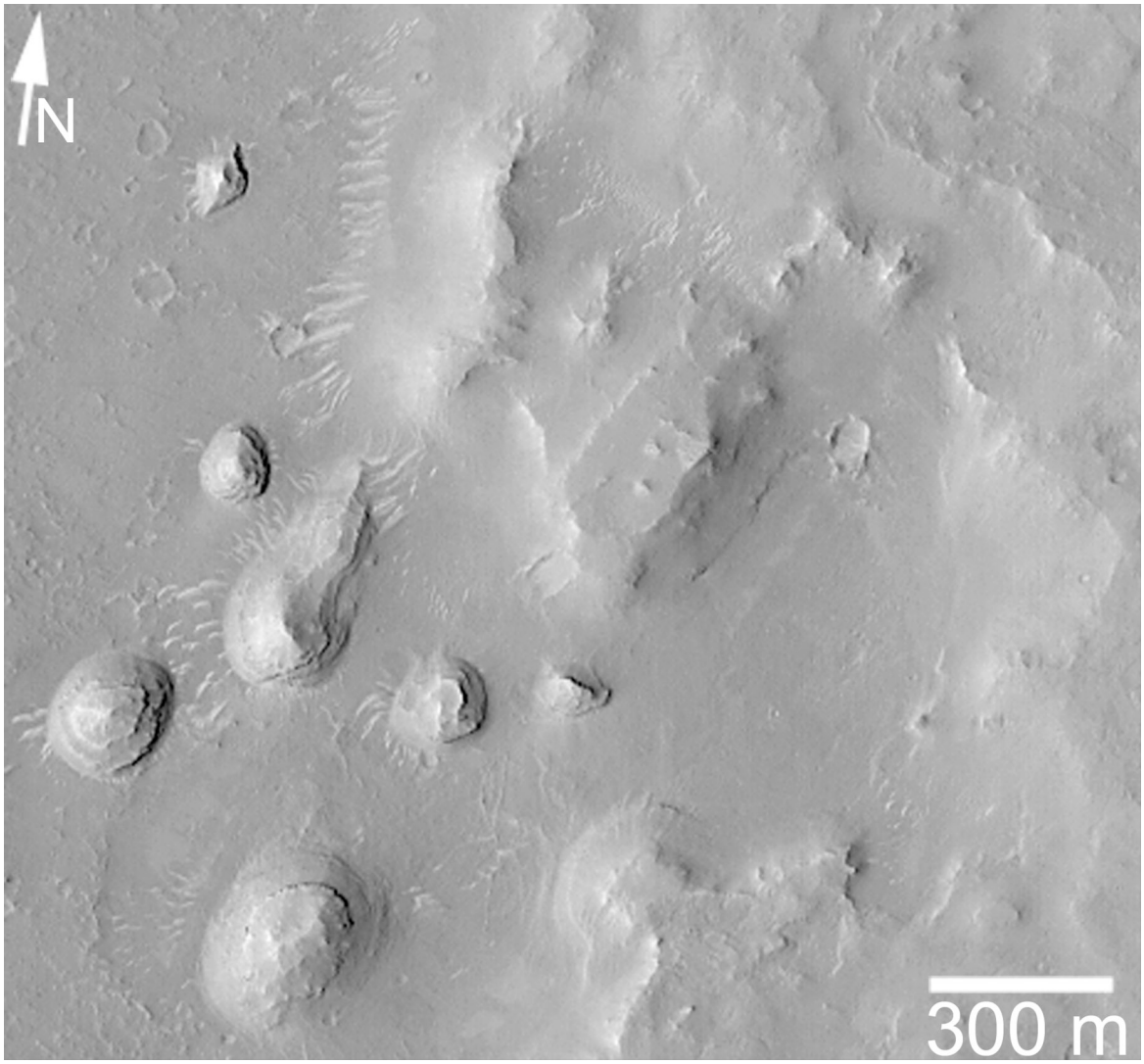

Figure 13. Example of layered intercrater plains in western Arabia Terra. Buttes exhibit multiple layers. MOC image M03-07310, near 9.8°N, 3.0°W, is illuminated from the left/bottom left.

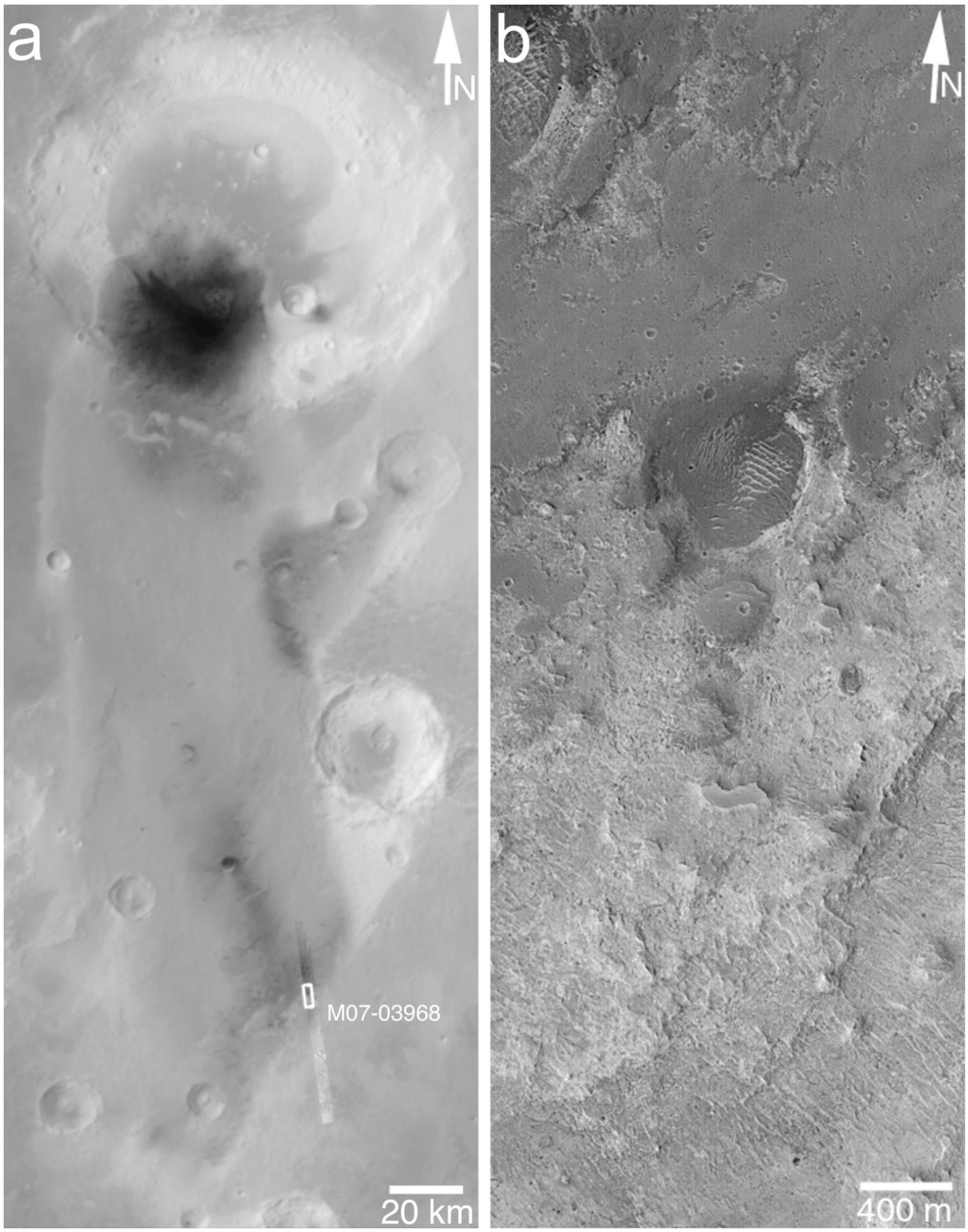

Figure 14. Coincidental occurrence of dark mesa-forming material and underlying light-toned substrate at the southeast margin of the Rutherford Crater wind streak. Unlike most west Arabia streaks, the streak from Rutherford Crater is, along its southeastern margin, superposed on a surface that was not previously mantled and thus reveals the nature of the terrain beneath the mantles that cover most of western Arabia Terra's intercrater terrain. **(a)** Context view of Rutherford Crater and its streak with the location of the high resolution view indicated. Image MOC M01-00459 is illuminated from the left. **(b)** High-resolution view of dark mesa-forming material (top third of image) and light-toned layered units (bottom two thirds of image) at the margin of Rutherford's dark streak. Image MOC M07-03968 is illuminated from the bottom left, located near 15.6°N, 10.3°W.

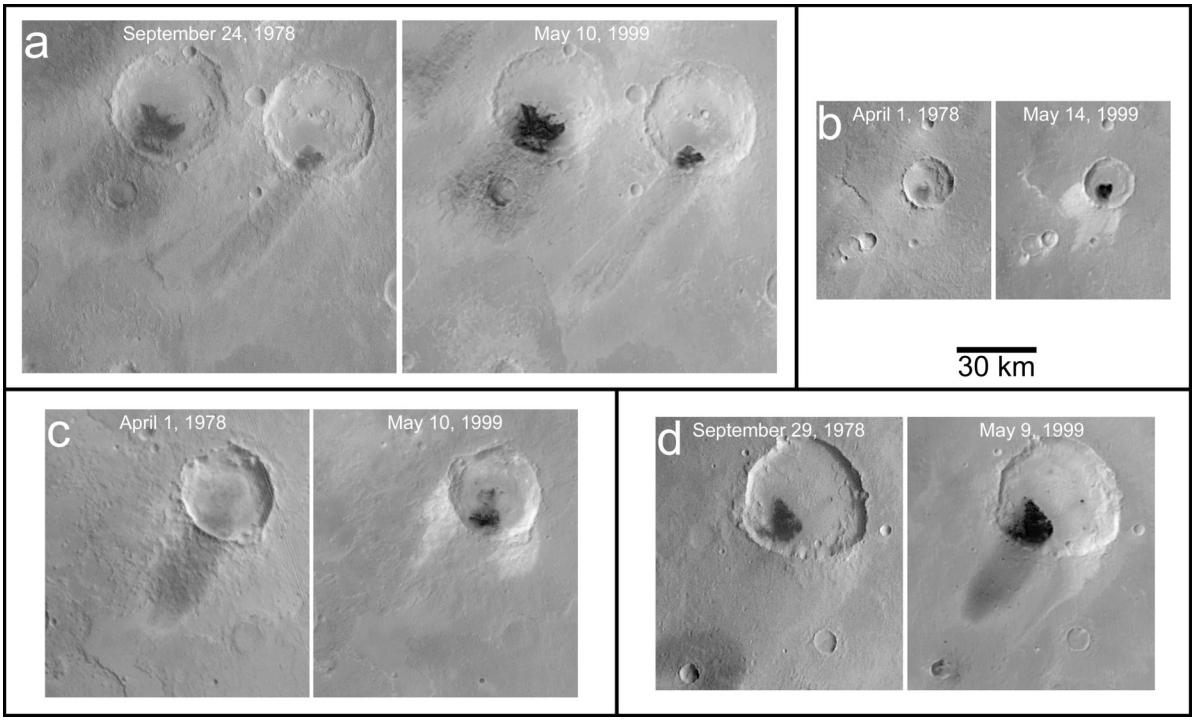

Figure 15. Variety of wind streak changes in western Arabia observed between Viking red filter images from 1978 and MOC red wide-angle images from 1999. **(a)** Images 829A43 and M01-00847, center near 10.4°N, 6.9°W. Some streaks remained largely unchanged, these two have only slightly different configurations between 1978 and 1999. **(b)** Images 653A62 and M01-01629, at 5.9 N, 356.2 W. Some streaks became brighter relative to their surroundings. **(c)** Images 653A58 and M01-00847, at 4.2°N, 5.4°W. Some streaks largely disappeared. **(d)** Images 831A18 and M01-00641, at 7.3°N, 353.2°W. Some streaks grew longer and/or darker. Illumination is from the right in the Viking images and from the left in the MOC images.

wind direction implied by the streak. In a few locations, there are superposed on the dark streaks some small (a few kilometers long, at most) bright wind streaks and tails in the lee of smaller craters and obstacles (Figure 16); these streaks and tails indicate that there has been some eolian transport at ground level, probably removal of bright dust coatings that might from time to time obscure part or all of a given streak (e.g., Figure 15c). Most of the dark streaks are underlain by thick mantles, but the streaks seem to be thin veneers (at least at their margins). Figure 17 shows a case in which there is no discernable difference in mantle thickness (nor the population of ridged and pitted surfaces found at this location) between the streak surface and terrain surrounding the streak, a relationship implying that dark streak material is a thin covering relative to the scale of a MOC image (i.e., << 1 m).

Eolian Activity

Eolian activity has long been presumed to be the primary cause for changes in western Arabia streak albedo, length, and configuration (Sagan et al. 1973, Thomas and Veverka 1979). Given that these changes are known to occur over periods as short as a few Earth years, evidence for eolian activity during the September 1997 to June 2001 period in western Arabia was sought.

Dust

Dust devils and dust plumes are excellent evidence for present-day eolian activity. Martian dust events range in size from small plumes of only a few kilometers in size up to global-scale events. Through June 2001, no global dust events were observed by MGS (although by the first week of July 2001, the MOC team realized that dust-raising events elsewhere on the planet that began in late June 2001 were becoming a global event (Cantor et al. 2001a)), and no dust storms large enough to be spotted by the MOC's 7500 m/pixel daily global images were detected in western Arabia Terra (Cantor et al. 2001b). Thus a search for smaller, localized dust events was conducted by examining all of the several hundred NA images and the highest-resolution WA images (~240 m/pixel) of the region. Most of the full-resolution WA images are ~115 x ~115 km square context views taken at the same time that a NA image was obtained. Other full-resolution WA pictures were acquired during the Geodesy Campaign in May 1999 (Caplinger and Malin 2001).

Dust devils on Mars were recorded from orbit by the Viking orbiters and the MOC NA and WA cameras (Thomas and Gierasch 1985, Malin and Edgett 2001). Full-resolution WA images have captured dust devils in a few locations where they are known to grow to sizes large enough to be seen by these cameras (Malin and Edgett 2001). None of the WA or NA images of western Arabia included a dust devil. However, filamentary streaks attributed by Malin and Edgett (2001) to the disruption and/or removal of thin surface coatings of dust by the passage of dust devil vortices are observed in NA images of some dune fields in western Arabia (Figure 18). In other locations on Mars, dust devils have been caught in the act of creating thin filamentary streaks; the streak patterns can change completely over intervals of a few months to an Earth year (Malin and Edgett 2001). The latter suggests that the streaks in Figure 18 were probably recent (a few months old at most) at the times the pictures were acquired.

Dust plumes caused by wind are expected to occur in western Arabia because a Viking orbiter image showed a few plumes rising from an intercrater surface a few tens of kilometers south of the southernmost west Arabia wind streaks in April 1978 (Figure 12). Some clouds connected to large dust storms on the northern plains obscured portions of northwestern Arabia Terra in WA pictures acquired 8–14 May 1999, 14 October 1999, and 30 March 2000 (see images M01-00461, M01-00641, M01-01030, M01-01032, M01-01238, M01-01240, M01-01446, M01-01631, M08-03018, M13-02172, M13-02174), but there were no plumes rising from western Arabia surfaces in any MOC images.

Dunes

The lack of observed dust activity in western Arabia may suggest that very little eolian activity (except occasional dust devils, Figure 18) occurred in the region during the MGS mission. Another approach to assessing eolian activity is to check the intracrater dune fields for movement. Smaller dunes, such as barchans of a few to a few tens of meters in planform dimensions, typically move faster than large dunes (Gay 1999) and thus would be the best candidates to examine for change. As noted above, there was no sign of change between September 1999 and September 2000 in the dune field in Figure 4. Likewise, Malin and Edgett (2001, Fig. 40) detected no change in a western Arabia dune field over an interval spanning May 1978 (Viking image 709A42) to December 1999 (MOC image M10-02916). The following MOC image pairs were also examined: (1) SP2-53203 and E05-01291, (2) SP2-44207 and M04-01484, (3) SP2-40803 and M11-01425, and (4) M07-01459 and E05-02646; no changes in dune position, shape, or slip faces were observed in these cases.

Discussion

Particle Size of Streak Sediment

Western Arabia Terra wind streaks are mantles composed of a material that is not as dark as the dunes and interdune surfaces from which the streaks emanate. The simplest explanation for this observation is that they consist of grains finer than and shed from the dunes and their subjacent, interdune terrain. In other words, MOC observations most strongly support the suspension deposition model for the genesis of the western Arabia streaks.

What are the suspendable, dark granular materials? On Earth, the answer would be "silt." Earth's dunes are composed mainly of grains that saltate under normal wind conditions, i.e., sand (Ahlbrandt 1979). The grains

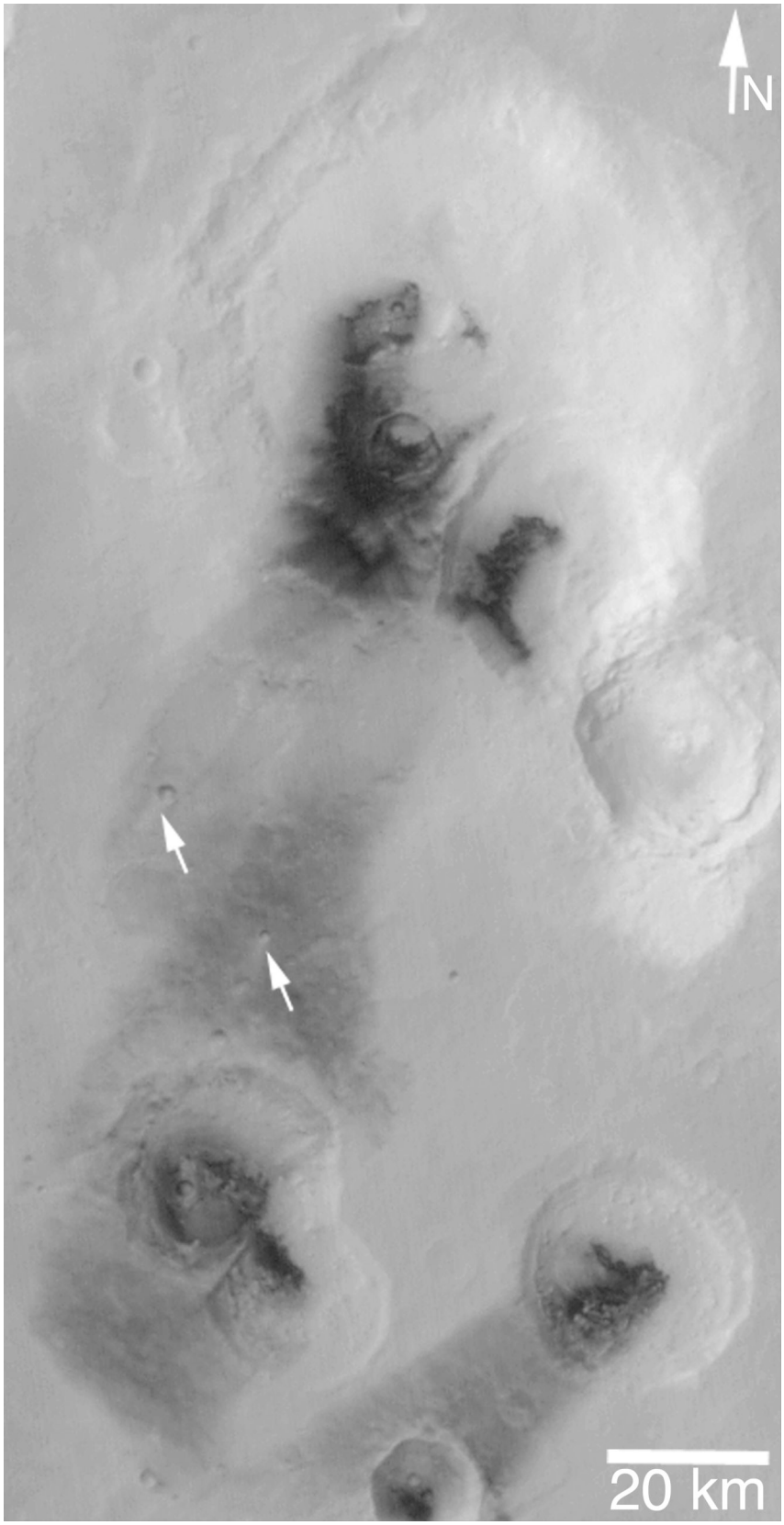

Figure 16. MOC image M01-01238, illuminated from the left. Some dark streaks in western Arabia exhibit evidence of surface and near-surface eolian transport. In this case, light-toned wind streaks in the lee of kilometer-scale impact craters (arrows) are superposed on the larger dark streak surface. Crater at top center is located at 10.8°N, 1.4°W.

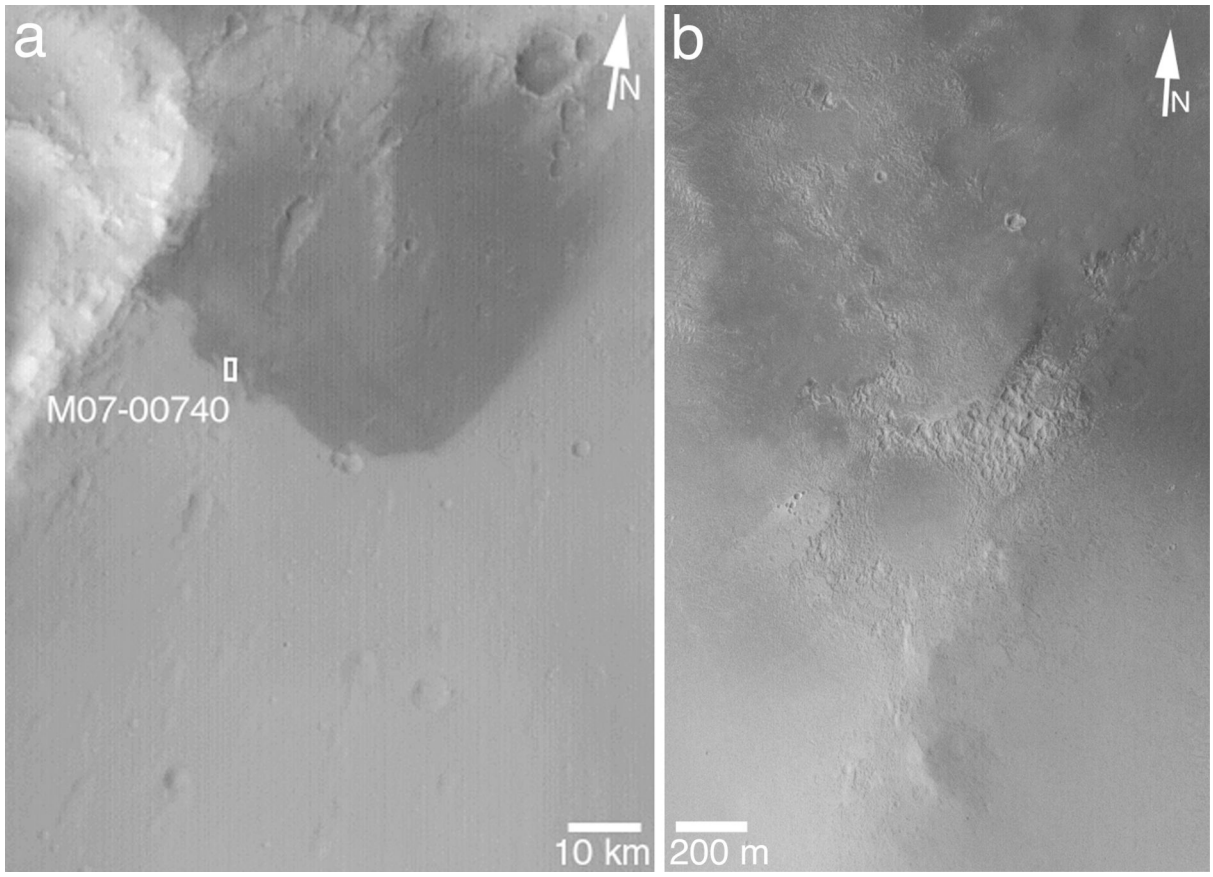

Figure 17. Most western Arabia Terra dark streaks appear at MOC NA image scales to be thin veneers superposed on a previously mantled surface. **(a)** MOC WA context image M07-00741 showing location of NA subframe at margin of dark streak near 8.8°N, 346.9°W. **(b)** NA image M07-00740 of streak margin. There is little difference between the light and dark mantle surfaces except their albedo. Both images are illuminated from the lower left.

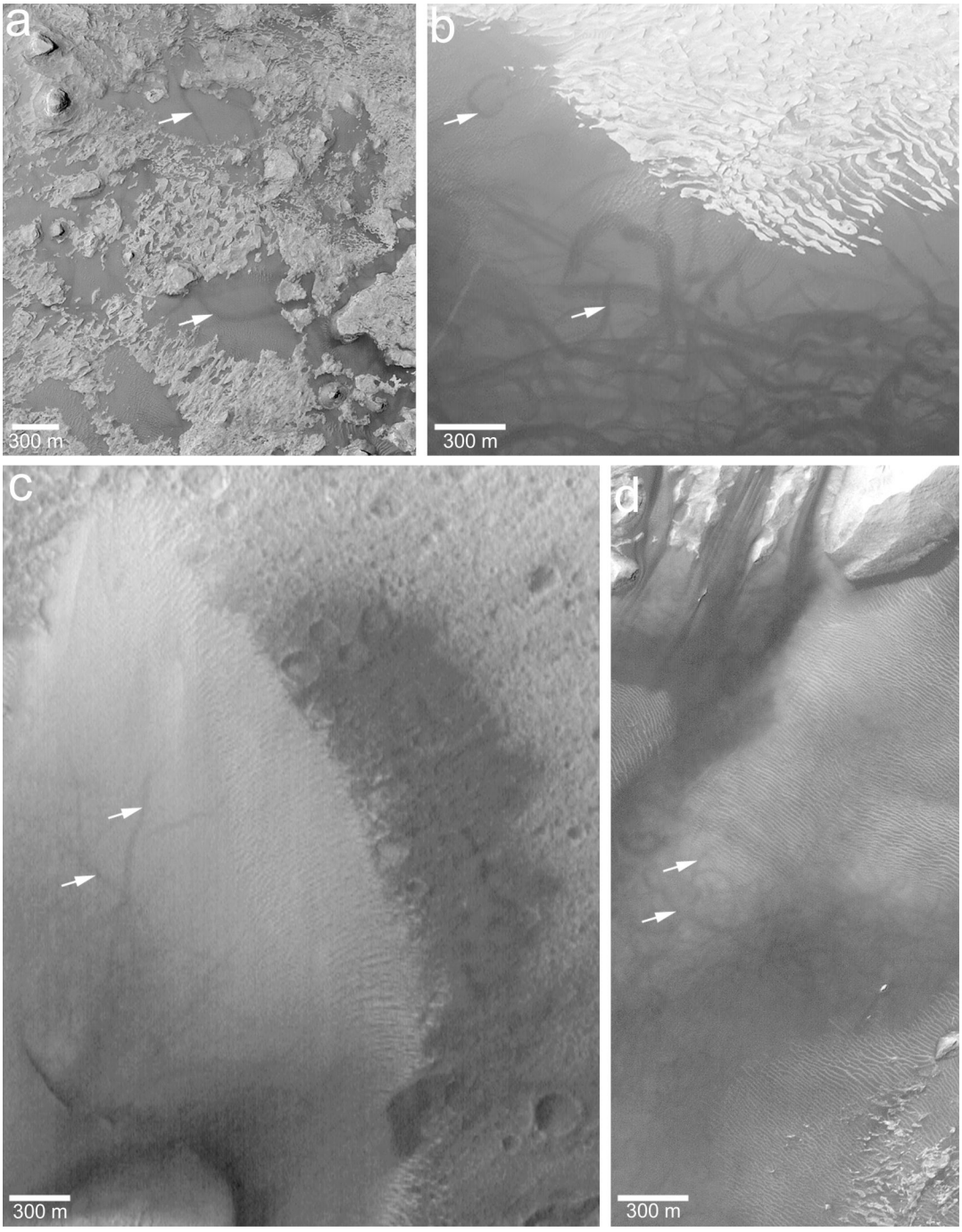

Figure 18. Dark filamentary streaks on intracrater dune surfaces in western Arabia Terra providing good evidence that dust devils have passed through the region. Multiple streaks are present in each image, a few examples are indicated by arrows. **(a)** Streaks on low patches of dark sand in MOC image E05-00661, near 2.7°N, 9.9°W. **(b)** Streaks on dune in crater near 8.2°N, 7.3°W; M20-00535. **(c)** Streaks on relatively light toned dune in Trouvelot Crater near 16.3°N, 13.4°W; SP2-53203; 16.3°N, 13.0°W. **(d)** Streaks on rippled dune in crater at 2.4°N, 9.3°W; M19-00188. Each picture is illuminated from the left, north is toward the top right.

suspended and carried away from dune fields on Earth are usually silt- and clay-sized. Plumes of fine grains rising from dune fields and their interdune surfaces on windy days is a common sight on Earth (e.g., Figure 3); indeed, the author has directly observed such events during the conduct of field investigations among dunes in Christmas Lake Valley, Oregon, in 1990–1994 (Edgett 1994). In the Oregon case, silt- and clay-sized sediments were observed being stripped from crusted, layered, interdune surfaces by clouds of saltating sand snaking along the ground and impacting a silt- and clay-rich substrate. Dunes can also contribute fine grains to suspension if these materials have previously settled on the dunes, infiltrated into them, and then later became exposed by wind on the erosional (stoss) slope of the dune. Saltating sand is a very effective mechanism for launching otherwise more cohesive (and thus more resistant to entrainment) silt- and clay-sized particles into suspension (e.g., Houser and Nickling, 2001). Coarser material raised into suspension from such dune fields (e.g., coarse silt) does not stay suspended for long; these grains are typically deposited within a few to several tens of kilometers from the source (Pye 1995).

Terrestrial experience suggests that there may be a population of low-albedo silt on Mars that can be raised into suspension and deposited to form the dark streaks of western Arabia Terra. While a few observations made prior to MGS hinted that silt-sized (or finer) dark material might exist on Mars (Dollfus and Deschamps 1986, McEwen 1992, Dollfus et al. 1993, Herkenhoff and Vasavada 1999), suspended Martian sediments were always assumed to be bright dust, and the subject of low-albedo grains that could be transported in suspension was not addressed in reviews regarding surface properties and eolian materials by Christensen and Moore (1992) or Greeley et al. (1992).

Are the western Arabia wind streaks composed of low-albedo silt? The answer is a qualified "yes." The qualifier stems from two other facts that suggest it is also possible that very fine sand (grains 62.5–125 μm) and fine sand (grains 125–250 μm) might also occur in the streaks. Studies of the thermal inertia of wind streaks in western Arabia Terra and similar streaks near Marte Vallis (e.g., the Pettit Crater streak) show their thermophysical properties are best interpreted as indicators of the presence of fine sand (Zimbelman 1986, Henry and Zimbelman 1988, Mellon et al. 2000, Pelkey et al. 2001). This conclusion may seem at odds with the interpretation that the streaks are composed of material transported in suspension. However, Mars is different from Earth, and it is possible that very fine and fine sand can be transported (for short distances) in suspension. Edgett and Christensen (1991) and Edgett and Christensen (1994) summarized empirical studies of Martian threshold friction velocity for particulate materials under modern conditions (e.g., atmospheric pressure ~6.5 millibars, gravity ~0.38 of Earth's) and noted that grains as large as 210 μm have the potential to become briefly suspended. While the atmosphere is thinner, the greater initial velocity of the grain, coupled with the lower gravity, lead to a longer saltation path length such that grains smaller than ~210 μm have path lengths that begin to approach infinity. Edgett and Christensen (1994 Fig. 8) show that there is a range of particle sizes from ~50 μm (silt) to ~210 μm (fine sand) that may be subject to short-term suspension at friction velocities at or just above threshold. Thus it is possible that the wind streaks are both formed from sediment transported in suspension and composed of particles that include some in the very fine and fine sand ranges.

Puzzles

While the western Arabia wind streaks appear to be the result of deposition from eolian suspension, three puzzles remain. The first is the origin of the bright margins around the streaks, the second regards the dramatic changes that have been observed to occur over the years (e.g., Figure 15, Veverka et al. (1977)), the third is the connection to eroded layered units found within the craters.

Bright Margins

The bright margins do not occur around all of the western Arabia streaks, but many of them do have these margins. The bright margins seem, in MOC images, to be extremely thin coatings, as noted for the type example (Figure 4f). The material comprising bright margins is probably dust. In a suspension deposition model for genesis of the western Arabia wind streaks, this dust would be the last material to settle of out a plume of suspended fines as they are removed from the dune field and crater floor located upwind. This explanation is not entirely satisfying, however, because if bright dust is the last material to settle out of suspension, then it should also settle upon the dark wind streaks and obscure them.

Changes in Streak Appearance

Changes in streak appearance over periods of years and decades (Figure 15) might be connected to the problem of bright margins. As noted, bright dust should settle upon and obscure the dark streak as the suspended sediment plume finally settles onto the surface. Perhaps this is what has caused obscuration of some streaks that were visible in the 1970s but not visible in 1997–2001 (Figure 15c). Perhaps some plumes of fine grains removed from crater floors and dune fields have more bright dust, and some have less. Some have more dark silt and very fine sand, and some have less. These would be modulated by the nature of the dust-raising event (wind velocity, duration, etc.) and the nature of sources for grains small enough to be suspended in a given western Arabia Terra Crater (dunes, layer outcrops, dust storm fallout).

Relation to Layered Units

What is the source of dune- and streak-forming sediment? Western Arabia differs from other regions because of its abundance of long, dark, depositional wind streaks. The region also differs from most because many of its craters exhibit exposures of eroded, layered material (e.g., Figures 6–9). It is therefore possible

that some fraction of the material comprising the layers in these craters is contributing sediment (via weathering and erosion) to the dune fields and wind streaks. However, most of the layers are light-toned, and the few examples of dark-toned layers (Figure 9c) are not as dark as the dunes within the same crater. This difference might be an indicator that such dark layers do not supply sediment to the dunes and streaks, or that the dark layers observed in outcrops are weathered (i.e., that a fresh surface exposed by a rock hammer would be found to be as dark as the dunes and/or wind streaks). The connection between dark streaks, dunes, and dark mesa-forming units (Figure 6) is likewise obscure. There are no clear cases in which sediment appears to be in the process of being shed from a dark mesa-forming unit. The source of sediment remains unknown, but proximity to eroded layered outcrops suggests there may be a connection.

Conclusions

The dark wind streaks of western Arabia each originate at a barchan dune field on a crater floor. The streaks consist of a relatively thin (< 1 m) coating of sediment deflated from the dunes and their vicinity. The bright margins of streaks are likewise thin. Crater floors from which the streaks emanate exhibit other erosional landforms, including remnants of once more extensive dark mesa-forming layers and thicker accumulations of light-toned layered material. Whether the latter two materials contribute sediment to the dunes or wind streaks is unknown. Wind-streak-forming sediments drape over a previous mantle that more thickly covers nearly all of western Arabia Terra; the surface of this regional mantle is the "dark red" unit known from Viking-era color studies. The wind streaks of western Arabia Terra consist of grains deposited from suspension. Under modern Martian conditions, these sediments could consist of silt, but thermophysical studies and eolian physics studies suggest that very fine and fine sand are also possible contributors. Despite the fact that the wind streaks are the result of eolian activity, and they have been observed to change over periods of years, no present activity in the form of dust plumes, dust devils, dust storms, or dune movement was detected between September 1997 and June 2001.

Acknowledgments. This material is based upon work supported by the National Aeronautics and Space Administration under contract NASW-99031 issued through the Office of Space Science, Mars Data Analysis Program. The manuscript benefited greatly from reviews and suggestions by M. A. Presley and P. C. Thomas.

References

Ahlbrandt, T. S. (1979) Textural parameters of eolian deposits, in *A Study of Global Sand Seas*, edited by E. D. McKee, *U. S. Geological Survey Professional Paper 1052*, 21–51.

Arvidson, R. E. (1974) Wind-blown streaks, splotches, and associated craters on Mars: Statistical analysis of Mariner 9 photographs, *Icarus 21*, 17–27, doi:10.1016/0019-1035(74)90086-4.

Arvidson, R. E., E. A. Guinness, M. A. Dale-Bannister, J. Adams, M. Smith, P. R. Christensen, and R. B. Singer (1989) Nature and distribution of surficial deposits in Chryse Planitia and vicinity, Mars, *Journal of Geophysical Research 94*(B2), 1573–1587, doi:10.1029/JB094iB02p01573.

Bagnold, R. A. (1941) *The Physics of Blown Sand and Desert Dunes*, Methuen, London.

Cantor, B. A., M. C. Malin, and K. S. Edgett (2001a) Martian dust events: A global view by MOC, abstract 34-01, *Bulletin of the American Astronomical Society 33*(3), 1097.

Cantor, B. A., P. B. James, M. Caplinger, and M. J. Wolff (2001b) Martian dust storms: 1999 Mars Orbiter Camera observations, *Journal of Geophysical Research 106*(E10), 23,653–23,687, doi:10.1029/2000JE001310.

Caplinger, M. A., and M. C. Malin (2001) The Mars Orbiter Camera Geodesy Campaign, *Journal of Geophysical Research 106*(E1), 23,595–23,606, doi:10.1029/2000JE001341.

Christensen, P. R. (1983) Eolian intracrater deposits: Physical properties and global distribution, *Icarus 56*, 496–518, doi:10.1016/0019-1035(83)90169-0.

Christensen, P. R. (1986) Regional dust deposits on Mars: Physical properties, age, and history, *Journal of Geophysical Research 91*(B3), 3533–3545, doi:10.1029/JB091iB03p03533.

Christensen, P. R. (1988) Global albedo variations on Mars: Implications for active aeolian transport, deposition, and erosion, *Journal of Geophysical Research 93*(B7), 7611–7624, doi:10.1029/JB093iB07p07611.

Christensen, P. R., and H. H. Kieffer (1979) Moderate resolution thermal mapping of Mars: The channel terrain around the Chryse basin, *Journal of Geophysical Research 84*(B14), 8233–8238, doi:10.1029/JB084iB14p08233.

Christensen, P. R., and H. J. Moore (1992) The Martian surface layer, in *Mars*, edited by H. H. Kieffer, B. M. Jakosky, C. W. Snyder, and M. S. Matthews, p. 686–729, University of Arizona Press, Tucson.

Cooper, C. D., and J. F. Mustard (1998) Rates of erosion in Oxia Palus, Mars, abstract 1164, *Lunar and Planetary Science XXIX*, Lunar and Planetary Institute, Houston, Texas.

Dollfus, A., and M. Deschamps (1986) Grain-size determination at the surface of Mars, *Icarus 67*, 37–50, doi:10.1016/0019-1035(86)90172-7.

Dollfus, A., M. Deschamps, and J. R. Zimbelman (1993) Soil texture and granulometry at the surface of Mars, *Journal of Geophysical Research 98*(E2), 3413–3429, doi:10.1029/92JE01502

Edgett, K. S. (1994) The volcaniclastic Shifting Sand Dunes of Christmas Lake Valley, Oregon, in *The Sand Component of the Modern Martian Aeolian Sedimentary System*, Ph.D. dissertation, p. 145–201, Arizona State University, Tempe.

Edgett, K. S. (1995) Physical properties of the Ares Valles (primary) and Trouvelot Crater (back-up) landing sites for Mars Pathfinder: Thermal inertia and rock abundance from Viking IRTM observations, *Lunar and Planetary Science XXVI*, 353–354, Lunar and Planetary Institute, Houston, Texas.

Edgett, K. S. and P. R. Christensen (1991) The particle size of martian aeolian dunes, *Journal of Geophysical Research 96*(E5), 22,765–22,776, doi:10.1029/91JE02412.

Edgett, K. S. and P. R. Christensen (1994) Mars aeolian sand: Regional variations among dark-hued crater floor features, *Journal of Geophysical Research 99*(E1), 1997–2018, doi:10.1029/93JE03094.

Edgett, K. S., and M. C. Malin (2000) New views of Mars eolian activity, materials, and surface properties: Three vignettes

from the Mars Global Surveyor Mars Orbiter Camera, *Journal of Geophysical Research 105*(E1), 1623–1650, doi:10.1029/1999JE001152.

Edgett, K. S., and T. J. Parker (1997) Water on early Mars: Possible subaqueous sedimentary deposits covering ancient cratered terrain in western Arabia Terra and Sinus Meridiani, *Geophysical Research Letters 24*(22), 2897–2900, doi:10.1029/97GL02840.

Gay, S. P., Jr. (1999) Observations regarding the movement of barchan sand dunes in the Nazca to Tanaca area of southern Peru, *Geomorphology 27*(3–4), 279–293, doi:10.1016/S0169-555X(98)00084-1.

Gill, T. E., D. L. Westphal, G. Stephens, and R. E. Peterson (2000) Integrated assessment of regional dust transport from west Texas and New Mexico, Spring 1999, Paper presented at *11th Joint Conference on the Applications of Air Pollution Meteorology with the Air and Waste Management Association*, American Meteorological Society, Boston, Massachusetts.

Golombek, M. P., H. J. Moore, and T. J. Parker (1997) Selection of the Mars Pathfinder landing site, *Journal of Geophysical Research 102*(E2), 3967–3988, doi:10.1029/96JE03318.

Greeley, R. (1986) Aeolian landforms: Laboratory simulations and field studies, in *Aeolian Geomorphology*, edited by W. G. Nickling, p. 195–211, Allen and Unwin, Winchester, Massachusetts.

Greeley, R., and J. D. Iversen (1985) *Wind as a Geological Process on Earth, Mars, Venus, and Titan*, Cambridge University Press, New York.

Greeley, R., J. D. Iversen, J. B. Pollack, N. Udovich, and B. White (1974a) Wind tunnel studies of martian aeolian processes, *Proceedings of the Royal Society, London, Series A* 341, 331–360, doi:10.1098/rspa.1974.0191.

Greeley, R., J. D. Iversen, J. B. Pollack, N. Udovich, and B. White (1974b) Wind tunnel simulations of light and dark streaks on Mars, *Science 183*, 847–849, doi:10.1126/science.183.4127.847

Greeley, R., P. Christensen, and R. Carrasco (1989) Shuttle radar images of wind streaks in the Altiplano, Bolivia, *Geology 17*(7), 665–668, doi:10.1130/0091-7613(1989)017<0665:SRIOWS>2.3.CO;2.

Greeley, R., N. Lancaster, S. Lee, and P. Thomas (1992) Martian aeolian processes, sediments, and features, in *Mars*, edited by H. H. Kieffer, B. M. Jakosky, C. W. Snyder, and M. S. Matthews, p. 730–766, University of Arizona Press, Tucson.

Henry, L. Y., and J. R. Zimbelman (1988) Physical properties and aeolian features in the Oxia Palus and Margaritifer Sinus Quadrangles of Mars, *Lunar and Planetary Science XIX*, 479–480.

Herkenhoff, K. E., and A. R. Vasavada (1999), Dark material in the polar layered deposits and dunes on Mars, *Journal of Geophysical Research 104*(E7), 16,487–16,500, doi:10.1029/1998JE000589.

Houser, C. A., and W. G. Nickling (2001) The emission and vertical flux of particulate matter < 10 µm from a disturbed clay-crusted surface, *Sedimentology 48*(2), 255–267, doi:10.1046/j.1365-3091.2001.00359.x.

Hynek, B. M., and R. J. Phillips (2001) Evidence for extensive denudation of the Martian highlands, *Geology 29*(5), 407–410, doi:10.1130/0091-7613(2001)029<0407:EFEDOT>2.0.CO;2.

Iversen, J. D., and B. R. White (1982) Saltation threshold on Earth, Mars, and Venus, *Sedimentology 29*(1), 111–119, doi:10.1111/j.1365-3091.1982.tb01713.x.

Kieffer, H. H., P. A. Davis, and L. A. Soderblom (1981) Mars' global properties: Maps and applications, *Proceedings of Lunar and Planetary Science 12B*, 1395–1417.

Malin, M. C., and K. S. Edgett (2000) Sedimentary rocks of early Mars, *Science 290*, 1927–1937, doi:10.1126/science.290.5498.1927.

Malin, M. C., and K. S. Edgett (2001) The Mars Global Surveyor Mars Orbiter Camera: Interplanetary Cruise through Primary Mission, *Journal of Geophysical Research 106*(E10), 23,429–23,570, doi:10.1029/2000JE001455.

Maxwell, T. A., and F. El-Baz (1982) Analogs of Martian eolian features in the western desert of Egypt, in *Desert Landforms of Southwest Egypt: A Basis for Comparison With Mars*, edited by F. El-Baz and T. A. Maxwell, *NASA Contractor Report CR-3611*, 247–259.

McCord, T. B., R. B. Singer, B. R. Hawke, J. B. Adams, D. L. Evans, J. W. Head, P. J. Mouginis-Mark, C. M. Pieters, R. L. Huguenin, and S. H. Zisk (1982) Mars: Definition and characterization of global surface units with emphasis on composition, *Journal of Geophysical Research 97*(B12), 10,129–10,148, doi:10.1029/JB087iB12p10129.

McEwen, A. S. (1987) Mars as a planet, *Lunar and Planetary Science XVIII*, 612–613, Lunar and Planetary Institute, Houston, Texas.

McEwen, A. S. (1989) Mars' global color and albedo, *Lunar and Planetary Science XX*, 660–661, Lunar and Planetary Institute, Houston, Texas.

McEwen, A. S. (1992) Temporal variability of the surface and atmosphere of Mars: Viking orbiter color observations, *Lunar and Planetary Science XXIII*, 877–878, Lunar and Planetary Institute, Houston, Texas.

Mellon, M. T., B. M. Jakosky, H. H. Kieffer, and P. R. Christensen (2000) High-resolution thermal inertia mapping from the Mars Global Surveyor Thermal Emission Spectrometer, *Icarus 148*, 437–455, doi:10.1006/icar.2000.6503.

Mustard, J. F. (1997) Are dark red soils and bright dust on Mars related through mineralogic phase changes? *Lunar and Planetary Science XXVI*, 1021–1022, Lunar and Planetary Institute, Houston, Texas.

Pelkey, S. H., B. M. Jakosky, and M. T. Mellon (2001) Thermal inertia of crater-related wind streaks on Mars, *Journal of Geophysical Research 106*(E10), 23,909–23,920, doi:10.1029/2000JE001433.

Peterfreund, A. R. (1981) Visual and infrared observations of wind streaks on Mars, *Icarus 45*, 447–467, doi:10.1016/0019-1035(81)90046-4.

Pollack, J. B., M. E. Ockert-Bell, and M. K. Shepard (1995), Viking lander image analysis of Martian atmospheric dust, *Journal of Geophysical Research 100*(E3), 5235–5250, doi:10.1029/94JE02640.

Presley, M. A. (1986) *The origin and history of surficial deposits in the central equatorial region of Mars*, M.S. thesis, 77 p., Washington University, St. Louis, Missouri.

Presley, M. A., and R. E. Arvidson (1988) Nature and origin of materials exposed in the Oxia Palus–Western Arabia–Sinus Meridiani region, Mars, *Icarus 75*, 499–517, doi:10.1016/0019-1035(88)90160-1.

Pye, K. (1995) The nature, origin and accumulation of loess, *Quaternary Science Reviews 14*(7–8), 653–667, doi:10.1016/0277-3791(95)00047-X.

Sagan, C., J. Veverka, P. Fox, R. Dubisch, J. Lederberg, E. Levinthall, L. Quam, R. Tucker, J. B. Pollack, and B. A. Smith (1972) Variable features on Mars: Preliminary

Mariner 9 television results, *Icarus 17*, 346–372, doi:10.1016/0019-1035(72)90005-X.

Sagan, C., J. Veverka, P. Fox, R. Dubisch, R. French, P. Gierasch, L. Quam, J. Lederberg, E. Levinthal, R. Tucker, B. Eross, and J. B. Pollack (1973) Variable features on Mars, 2, Mariner 9 global results, *Journal of Geophysical Research 78*(20), 4163–4196, doi:10.1029/JB078i020p04163.

Sagan, C., D. Pieri, P. Fox, R. E. Arvidson, and E. A. Guinness (1977) Particle motion on Mars inferred from the Viking lander cameras, *Journal of Geophysical Research 82*(28), 4430–4438, doi:10.1029/JS082i028p04430.

Schaber, G. G. (1980) Radar, visual, and thermal characteristics of Mars: Rough planar surfaces, *Icarus 42*, 159–184, doi:10.1016/0019-1035(80)90070-6.

Sharp, R. P. (1963) Wind ripples, *Journal of Geology 71*(5), 617–636, doi:10.1086/626936.

Singer, R. B., E. Cloutis, T. L. Roush, P. J. Mouginis-Mark, B. R. Hawke, and P. R. Christensen, Multispectral analysis of the Kasei Vallis–Lunae Planum region, Mars, *Lunar and Planetary Science XV*, 794–795, Lunar and Planetary Institute, Houston, Texas.

Soderblom, L. A., K. Edwards, E. M. Eliason, E. M. Sanchez, and M. P. Charette (1978) Global color variations on the Martian surface, *Icarus 34*, 446–464, doi:10.1016/0019-1035(78)90037-4.

Strickland, E. L. (1989) Physical properties of Oxia/Lunae Planum and Arabia-type units in the central equatorial region of Mars, *Lunar and Planetary Science XX*, 1079–1080, Lunar and Planetary Institute, Houston, Texas.

Thomas, P. (1984) Martian intracrater splotches: Occurrence, morphology, and colors, *Icarus 57*, 205–227, doi:10.1016/0019-1035(84)90066-6.

Thomas, P., and P. J. Gierasch (1985) Dust devils on Mars, *Science 230*, 175–177, doi:10.1126/science.230.4722.175.

Thomas, P., and J. Veverka (1979) Seasonal and secular variation of wind streaks on Mars: An analysis of Mariner 9 and Viking data, *Journal of Geophysical Research 84*(B14), 8131–8146, doi:10.1029/JB084iB14p08131.

Thomas, P., and J. Veverka (1986) Red/violet contrast reversal on Mars: Significance for eolian sediments, *Icarus 66*, 39–55, doi:10.1016/0019-1035(86)90005-9.

Thomas, P., J. Veverka, S. Lee, and A. Bloom (1981) Classification of wind streaks on Mars, *Icarus 45*, 124–153, doi:10.1016/0019-1035(81)90010-5.

Tomasko, M. G., L. R. Doose, M. Lemmon, P. H. Smith, and E. Wegryn (1999) Properties of dust in the Martian atmosphere from the imager on Mars Pathfinder, *Journal of Geophysical Research 104*(E4), 8987–9007, doi:10.1029/1998JE900016.

Veverka, J., P. Thomas, and R. Greeley (1977) A study of variable features on Mars during the Viking Primary Mission, *Journal of Geophysical Research 82*(28), 4167–4187, doi:10.1029/JS082i028p04167.

Wentworth, C. K. (1922) A scale of grade and class terms for clastic sediments, *Journal of Geology 30*(5), 377–392, doi:10.1086/622910.

Wyatt, M. B., J. L. Bandfield, H. Y. McSween Jr., and P. R. Christensen (2001) Compositions of low albedo intracrater materials and wind streaks on Mars: Examination of MGS TES data in western Arabia Terra, abstract 1872, *Lunar and Planetary Science XXXII*, Lunar and Planetary Institute, Houston, Texas.

Zimbelman, J. R. (1986) Surface properties of the Pettit wind streak on Mars: Implications for sediment transport, *Icarus 66*, 83–93, doi:10.1016/0019-1035(86)90008-4.

Zimbelman, J. R., and R. Greeley (1982) Surface properties of ancient cratered terrain in the northern hemisphere of Mars, *Journal of Geophysical Research 87*(B12), 10,181–10,189, doi:10.1029/JB087iB12p10181.

Zimbelman, J. R., and H. H. Kieffer (1979) Thermal mapping of the northern equatorial and temperate latitudes of Mars, *Journal of Geophysical Research 84*(B14), 8239–8251, doi:10.1029/JB084iB14p08239.

Zimbelman, J. R., and S. H. Williams (1996) Wind streaks: Geological and botanical effects on surface albedo contrast, *Geomorphology 17*(1–3), 167–185, doi:10.1016/0169-555X(95)00098-P.

Zimbelman, J. R., S. H. Williams, and V. P. Tchakerian (1995) Sand transport paths in the Mojave Desert, southwestern United States, in *Desert Aeolian Processes*, edited by V. P. Tchakerian, p. 101–129, Chapman and Hall, New York.

Differences between the © 2002 American Geophysical Union version of the paper and this one:

- The layout/formatting of the document.
- Figure 2 in the AGU version was a grayscale image with a color plate version of the figure provided elsewhere in the volume.
- Typographical errors in the published versions of Tables 1 and 2 have been herein corrected. Also, corrected latitude/longitude for first entry in Table 1.
- The reference citations are herein unabbreviated and include digital object identifiers (DOI) for documents for which a DOI was available as of 27 December 2009.
- 28 December 2009: Note that the URL for the Hubble Space Telescope image mentioned on page 1 is no longer active. (A cautionary tale about referencing URLs in scientific papers).